Physica D 481 (2025) 134803

Contents lists available at ScienceDirect

Physica D

journal homepage: www.elsevier.com/locate/physd

On the existence of traveling wave solutions for cold plasmas

Diego Alonso-Orán [a,*], Angel Durán [b], Rafael Granero-Belinchón [c]

[a] Departamento de Análisis Matemático y Instituto de Matemáticas y Aplicaciones (IMAULL), Universidad de La Laguna C/. Astrofísico Francisco Sánchez s/n, 38200 La Laguna, Spain

[b] Applied Mathematics Department, University of Valladolid, 47011 Valladolid, Spain

[c] Departamento de Matemáticas, Estadística y Computación, Universidad de Cantabria. Avda. Los Castros s/n, Santander, Spain

ARTICLE INFO

Communicated by Victor M. Perez–Garcia

Keywords:
Bifurcation theory
Traveling waves
Homoclinic orbits
Numerical generation

ABSTRACT

The present paper is concerned with the existence of traveling wave solutions of the asymptotic model, derived by the authors in a previous work, to approximate the unidirectional evolution of a collision-free plasma in a magnetic field. First, using bifurcation theory, we can rigorously prove the existence of periodic traveling waves of small amplitude. Furthermore, our analysis also evidences the existence of different type of traveling waves. To this end, we present a second approach based on the analysis of the differential system satisfied by the traveling wave profiles, the existence of equilibria, and the identification of associated homoclinic and periodic orbits around them. The study makes use of linearization techniques, normal forms, and numerical computations to show the existence of different types of traveling wave solutions, with monotone and non-monotone behavior and different regularity, as well as periodic traveling waves.

1. Introduction

The motion of a magnetized cold plasma consisting of singly-charged particles can be described by the following hyperbolic–hyperbolic–elliptic system of PDEs [1,2]

$$n_t + (un)_x = 0, \tag{1a}$$

$$u_t + uu_x + \frac{bb_x}{n} = 0, \tag{1b}$$

$$b - n - \left(\frac{b_x}{n}\right)_x = 0, \tag{1c}$$

where n represents the number density of ions, u is the ion velocity and b the magnetic field. In (1) the unknowns are functions of $(x,t) \in \mathbb{R}\times[0,\infty)$.

The system (1) was introduced in [2] to study hydromagnetic waves traveling across a magnetic field. Later studies regarding the oblique propagation of hydromagnetic waves were investigated in [1,3]. The rigorous justification of the KdV limit of (1) is provided in [4]. The first and third author showed in [5] the local well-posedness of classical solutions to (1) with initial data in $(\rho_0 - 1, u_0) \in H^2(\mathbb{R})\times H^3(\mathbb{R})$. Later, in [6], Bae, Choi and Kwon demonstrate that solutions to (1) blow-up in finite time for a certain class of initial data.

Recently in [7], by means a multi-scale expansion approach, the authors derived asymptotic models of (1). We make a brief description of it, see [7] for details. From the formal expansions

$$n = 1 + \sum_{\ell=0}^{\infty} \epsilon^{\ell+1} N^{(\ell)},\ b = 1 + \sum_{\ell=0}^{\infty} \epsilon^{\ell+1} B^{(\ell)},\ u = \sum_{\ell=0}^{\infty} \epsilon^{\ell+1} U^{(\ell)}, \tag{2}$$

then the first one is the nonlocal Boussinesq system

$$h_t + (hv)_x + v_x = 0, \tag{3a}$$

$$v_t + vv_x + [\mathscr{L}, \mathscr{N}h]\,h + \mathscr{N}h = 0, \tag{3b}$$

where the nonlocal operators are given by

$$\mathscr{L} = -\partial_x^2(1-\partial_x^2)^{-1},\ \mathscr{N} = \partial_x(1-\partial_x^2)^{-1}\ (\text{so } \partial_x\mathscr{N} = -\mathscr{L}), \tag{4}$$

with Fourier symbols

$$\widehat{\mathscr{L}h}(\xi) = \frac{\xi^2}{1+\xi^2}\hat{h}(\xi),\ \widehat{\mathscr{N}h}(\xi) = \frac{i\xi}{1+\xi^2}\hat{h}(\xi),$$

and where $[\mathscr{L},\cdot]\cdot$ denotes the commutator

$$[\mathscr{L}, f]\,g = \mathscr{L}(fg) - f\mathscr{L}g.$$

In (3) $h = \varepsilon N^{(0)} + \varepsilon^2 N^{(1)}$ and $v = \varepsilon U^{(0)} + \varepsilon^2 U^{(1)}$ represent, respectively, second-order approximations in a multi-scale expansion of the ionic density and ionic velocity variables. The additional assumption $U^{(0)} = N^{(0)}$, concerning the first-order terms of the expansions (2) leads to a second asymptotic model, in the form of a bi-directional non-local wave

* Corresponding author.
E-mail addresses: dalonsoo@ull.edu.es (D. Alonso-Orán), angeldm@uva.es (A. Durán), rafael.granero@unican.es (R. Granero-Belinchón).

https://doi.org/10.1016/j.physd.2025.134803
Received 13 October 2024; Received in revised form 2 June 2025; Accepted 5 June 2025
Available online 23 June 2025

equation for h which can be simplified, after some change of variables, to the single, scaled, unidirectional, nonlocal wave equation for h given by

$$h_t = -\frac{1}{2}\left(3hh_x - [\mathscr{L}, \mathscr{N}h]h - \mathscr{N}h - h_x\right). \tag{5}$$

Furthermore, besides the derivation of (3) and (5), the well-posedness of the corresponding initial-value problems (ivp's) and additional properties, such as the Hamiltonian structure

$$h_t = \frac{1}{2}\partial_x \delta E(h),$$

where $\delta E = \frac{\delta E}{\delta h}$ denotes the variational derivative and

$$E(h) = \frac{1}{2}\int_{-\infty}^{\infty}\left(h^2 - h^3 + (\mathscr{B}h)^2 + h(\mathscr{N}h)^2\right)dx,\ \mathscr{B} := (\mathrm{I} - \partial_{xx})^{-1/2},$$

existence of additional conserved quantities and the formation of singularities in finite time are also studied in [7].

Our next step in the analysis of (3) and (5) is concerned with the existence of traveling wave solutions. These are solutions of permanent form and traveling with some constant velocity. Their determination transforms (3) and (5) into the corresponding ordinary differential equations (odes) for the wave profiles, depending on the speed. If the profiles are known to go to zero asymptotically (surely along with their derivatives up to some order), that is, if the profiles are localized, they are usually called solitary waves. When the odes are complemented with periodic boundary conditions, the corresponding solutions (if they exist) are called periodic traveling waves. The present paper is focused on the existence of these two types of traveling waves for the unidirectional Eq. (5), while the system (3) will be considered in a forthcoming work.

The existence of solutions with special structure of partial differential equations is a classical topic in mathematical modeling. This is a natural consequence of the relevance of these solutions in the general dynamics of the model under study, [8], with particular emphasis on solitary, periodic or other forms of traveling waves, [9,10]. While the literature on waves in plasma and cold plasma models is extensive see, e. g. [11,12], the study of traveling waves, to our knowledge, seems to be focused on plane wave solutions (cf. [12,13] and references therein), which serves as motivation for the present paper.

The main contributions of the paper are the following:

- The first result is the existence of periodic traveling waves of small amplitude and $O(1)$ velocity, cf. [7]. The proof hinges on non-linear bifurcation techniques via Crandall–Rabinowitz theorem. The bifurcation approach to prove the existence of traveling waves for different equations has been used by different authors [14–17].
- We also show the existence of different types of traveling wave solutions of (5) (including, but not only, solitary waves). The approach is based on the application of normal form theory for reversible vector fields, [18–20], to the differential system for traveling wave profiles obtained from a reformulation of (5) with only local terms. Due to the lack of conclusive results in some parts, the discussion is supported by some experiments from an efficient numerical procedure to compute approximations to the profiles. The numerical results suggest some additional properties of the waves, concerning amplitude, speed and decay at infinity.

Plan of the paper

The paper is structured as follows. In Section 2 we fix the notation and present some auxiliary results on bifurcation theory. In Section 3 the existence of smooth periodic traveling waves of small amplitude is proved via a bifurcation argument. Section 4 is devoted to derive the local formulation of (5) and to identify the families of equilibria of the corresponding ode system satisfied by the traveling waves. For two of these equilibria and from the reversibility property of the differential equations, the existence of traveling wave solutions as homoclinic and periodic orbits around them is discussed in Section 5. The discussion is based on the application of normal form theory of the corresponding reversible vector fields, [20], with the help of literature for similar equations, (cf., among others, [18,19,21–23] and references therein), and the numerical experiments of generation of approximate waves. Some concluding remarks are outlined in Section 6. The numerical procedure to compute approximations of traveling wave profiles is described in Appendix.

2. Notation and auxiliary results

In this section, we fix the notation used throughout the paper and recall some classical results on bifurcation theory. For a periodic function f with values in $\mathbb{R}$ we define the Hölder norms as

$$\|f\|_{C^0(\mathbb{T})} = \sup_{x\in\mathbb{T}^1}|f|,\ \|f\|_{C^k(\mathbb{T})} = \|f\|_{C^0(\mathbb{T})} + \sum_{\ell=1}^{k}\left\|\partial_x^\ell f\right\|_{C^0(\mathbb{T})},\ k\in\mathbb{N},$$

$$\|f\|_{C^{0,\alpha}(\mathbb{T})} = \|f\|_{C^0(\mathbb{T})} + \sup_{x_1,x_2\in(\mathbb{T})}\frac{|f(x_1)-f(x_2)|}{|x_1-x_2|^\alpha},\ 0<\alpha<1,$$

$$\|f\|_{C^{k,\alpha}(\mathbb{T})} = \|f\|_{C^{k-1}(\mathbb{T})} + \left\|\partial_x^k f\right\|_{C^\alpha(\mathbb{T})},\ k\in\mathbb{N},\ 0<\alpha<1.$$

The Banach space of continuous functions for which the above norms are finite will be denoted $C^k(\mathbb{T})$ and $C^{k,\alpha}(\mathbb{T})$.

We denote by $\mathscr{Q} := (\mathrm{I} - \partial_{xx})^{-1}$ the Helmholtz operator with Fourier symbol

$$\widehat{\mathscr{Q}f}(\xi) = \frac{1}{1+\xi^2}\widehat{f}(\xi).$$

Acting on square integrable periodic functions f, the Helmholtz operator has the representation

$$\mathscr{Q}f(x) = [(\mathrm{I} - \partial_{xx})^{-1}]f(x) = [\mathsf{G}_{\mathbb{T}} \star f](x), \tag{6}$$

where the Green function $\mathsf{G}_{\mathbb{T}}$ is explicitly given by

$$\mathsf{G}_{\mathbb{T}}(x) = \frac{\cosh(x - 2\pi[\frac{x}{2\pi}] - \pi)}{2\sinh(\pi)}. \tag{7}$$

We have the following bound whose proof can be found in [24, Theorem 4, §4.4]:

Lemma 2.1. *The operator $\mathscr{Q}$ maps $C^{k,\alpha}(\mathbb{T})$ isomorphically onto $C^{k+2,\alpha}(\mathbb{T})$. More precisely, there exists a constant $C>0$ such that*

$$\|\mathscr{Q}f\|_{C^{k+2,\alpha}(\mathbb{T})} \le C\|f\|_{C^{k,\alpha}(\mathbb{T})},\quad f\in C^{k,\alpha}(\mathbb{T}),\quad k\in\mathbb{N}\cup\{0\}. \tag{8}$$

Therefore as a direct consequence the non-local operators in (4) written as

$$\mathscr{L} = -\partial_x^2\mathscr{Q},\ \mathscr{N} = \partial_x\mathscr{Q}. \tag{9}$$

enjoyed the following estimates

$$\|\mathscr{L}f\|_{C^{k,\alpha}(\mathbb{T})} \le C\|f\|_{C^{k,\alpha}(\mathbb{T})},\ \|\mathscr{N}f\|_{C^{k+1,\alpha}(\mathbb{T})} \le C\|f\|_{C^{k,\alpha}(\mathbb{T})}. \tag{10}$$

The previous bounds (8)–(10) are particular cases of a more general theory of mapping properties for pseudo-differential operators in Besov spaces, cf. [25, Theorem 6.19, §6.6].

Next, let us revisit the Crandall–Rabinowitz Theorem, an essential tool in bifurcation theory that we will use to show the existence of smooth periodic traveling waves. Before we dive in, let us first go over the following definition:

Definition 1 (*Fredholm Operator*)**.** Let X and Y be two Banach spaces. A continuous linear mapping $T : X \to Y$, is a Fredholm operator if it fulfills the following properties,

(1) $\dim \mathrm{Ker}\, T < \infty$,
(2) $\mathrm{Im}\, T$ is closed in Y,

(3) codim $\operatorname{Im} T < \infty$.

The integer $\dim \operatorname{Ker} T - \operatorname{codim} \operatorname{Im} T$ is called the Fredholm index of T. Moreover, we also remark that the index of a Fredholm operator remains unchanged under compact perturbations, cf. [26,27]. Next, let us state the classical Crandall–Rabinowitz theorem [28] which reads as follows:

Theorem 1 (*Crandall–Rabinowitz Theorem*). *Let X, Y be two Banach spaces, V be a neighborhood of 0 in X and $F : \mathbb{R} \times V \to Y$ be a function with the properties,*

(1) *$F(\lambda, 0) = 0$ for all $\lambda \in \mathbb{R}$.*
(2) *The partial derivatives $\partial_\lambda F$, $\partial_f F$ and $\partial_\lambda \partial_f F$ exist and are continuous.*
(3) *The operator $\partial_f F(\lambda_0, 0)$ is Fredholm of zero index and $\operatorname{Ker}(\partial_f F(\lambda_0, 0)) = \langle f_0 \rangle$ is one-dimensional.*
(4) *Transversality assumption: $\partial_\lambda \partial_f F(\lambda_0, 0) f_0 \notin \operatorname{Im}(\partial_f F(\lambda_0, 0))$.*

If Z is any complement of $\operatorname{Ker}(\partial_f F(\lambda_0, 0))$ in X, then there is a neighborhood U of $(\lambda_0, 0)$ in $\mathbb{R} \times X$, an interval $(-a, a)$, and two continuous functions $\Phi : (-a, a) \to \mathbb{R}$, $\beta : (-a, a) \to Z$ such that $\Phi(0) = \lambda_0$ and $\beta(0) = 0$ and

$$F^{-1}(0) \cap U = \{(\Phi(s), s f_0 + s\beta(s)) : |s| < a\} \cup \{(\lambda, 0) : (\lambda, 0) \in U\}.$$

3. Existence of periodic traveling wave solutions

This section is devoted to show the existence of smooth periodic traveling waves of small amplitude. The precise statement of result reads:

Theorem 2. *For any $m \geq 1$ there exists a one dimensional curve $s \mapsto (c_s, \varphi_s)$, with $s \in I$, such that*

$$h(x) = \varphi_s(x) \in C^{1,\alpha}([0, 2\pi], \mathbb{R}),$$

$$h \in X_m := \left\{ f \in C^{1,\alpha}([0, 2\pi]), \right.$$

$$\left. f(\xi) = \sum_{k \geq 1} f_k \cos(mk\xi) \text{ with norm} \|f\|_{X_m} = \|f\|_{C^{1,\alpha}} \right\},$$

and h is a traveling wave solution to (5) with constant speed c_s where

$$c_s \approx -\frac{1}{2} - \frac{1}{2(1+m^2)}.$$

We use the name $m-$fold traveling waves to denote traveling wave solutions to (5) with profiles in X_m.

3.1. Formulation and functional spaces

We look for periodic traveling waves for h and hence we make the Ansatz

$$h(x, t) = \varphi(x - ct),$$

for some speed $c \in \mathbb{R}$. Hence, plugging it into (5) we find the problem

$$-c\varphi' = -\frac{1}{2}\left(3\varphi\varphi' - [\mathscr{L}, \mathscr{N}\varphi]\varphi - \mathscr{N}\varphi - \varphi'\right). \tag{11}$$

As a consequence, the equation reduces to

$$F[c, \varphi](\xi) = 0, \quad \xi \in [-\pi, \pi],$$

where

$$F[c, \varphi](\xi) = \frac{1}{2}\left(3\varphi(\xi)\varphi'(\xi) - [\mathscr{L}, \mathscr{N}\varphi(\xi)]\varphi(\xi) - \mathscr{N}\varphi(\xi) - \varphi'(\xi)\right) - c\varphi'(\xi). \tag{12}$$

We observe that, regardless of the value of c we have the following line of trivial solutions

$$F[c, 0] = 0.$$

Following [14], we define the functional spaces

$$X := \left\{ h \in C^{1,\alpha}([0, 2\pi], \mathbb{R}), \quad h(\xi) = \sum_{k \geq 1} h_k \cos(k\xi) \text{ with norm } \|h\|_X = \|h\|_{C^{1,\alpha}} \right\},$$

$$Y := \left\{ h \in C^{0,\alpha}([0, 2\pi], \mathbb{R}), \quad h(\xi) = \sum_{k \geq 1} h_k \sin(k\xi) \text{ with norm } \|h\|_Y = \|h\|_{C^{0,\alpha}} \right\}.$$

Furthermore, we also introduce the space

$$Z := \left\{ h \in C^{2,\alpha}([0, 2\pi], \mathbb{R}), \quad h(\xi) = \sum_{k \geq 1} h_k \sin(k\xi) \text{ with norm } \|h\|_Z = \|f\|_{C^{2,\alpha}} \right\}.$$

It is straightforward to check that the embedding $Z \hookrightarrow Y$ is compact and the functions in X are zero-mean.

3.2. Spectral and transversality properties of the linearized operator

In this subsection, we will check that the hypothesis of the Crandall–Rabinowitz Theorem 1 are satisfied. To start with, let us show that the operator $F : \mathbb{R} \times X \to Y$ given in (12) is well-defined and $\mathscr{C}^1(\mathbb{R} \times X \to Y)$. We first observe that if φ is an even function, $\varphi(\xi) = \varphi(-\xi)$, then $F[c, \varphi]$ is an odd function (and as a consequence we only need to check the regularity to show that F maps X into Y), i.e.,

$$F[c, \varphi](\xi) = -F[c, \varphi](-\xi).$$

To that purpose, we first notice that $\varphi'(-\xi) = -\varphi'(\xi)$. Moreover, using the representation (6)–(7) for the Helmholtz operator, we easily check that

$$\mathscr{Q}\varphi(\xi) = \mathscr{Q}\varphi(-\xi).$$

Invoking (9) we find that

$$\mathscr{N}\varphi(\xi) = \mathscr{Q}\varphi'(\xi) = -\mathscr{N}\varphi(-\xi), \quad \mathscr{L}\varphi(\xi) = (\mathrm{I} - \mathscr{Q})\varphi(\xi) = \mathscr{L}\varphi(-\xi),$$

and hence $[\mathscr{L}, \mathscr{N}\varphi]\varphi(\xi) = -[\mathscr{L}, \mathscr{N}\varphi]\varphi(-\xi)$. Thus, by combining the previous identities and recalling (12) we conclude that $F[c, \varphi](\xi) = -F[c, \varphi](-\xi)$ satisfying the symmetry property.

In the following let us show that $F : \mathbb{R} \times X \to Y$ is well-defined. It is straightforward to check that

$$\left\| -\frac{1}{2}\left(\mathscr{N}\varphi + \varphi'\right) - c\varphi' \right\|_Y \leq C \|\varphi\|_X.$$

Similarly, the non-linear terms can be bounded by

$$\left\| \frac{1}{2}\left(3\varphi\varphi' - [\mathscr{L}, \mathscr{N}\varphi]\varphi\right) \right\|_Y \leq C \|\varphi\|_X \|\varphi\|_Y + \|\varphi\|_Y^2,$$

where we have used estimate (10) and the fact that

$$\|fg\|_Y \leq \|f\|_Y \|g\|_Y.$$

Thus, since $X \hookrightarrow Y$, we conclude that

$$\|F[c, \varphi]\|_Y \leq C\left(\|\varphi\|_X^2 + \|\varphi\|_X\right).$$

In order to prove that $F \in \mathscr{C}^1(\mathbb{R} \times X \to Y)$ it is sufficient to show that the Gateaux derivative of F verifies

$$\|\partial_\varphi F[c, \varphi_1]f - \partial_\varphi F[c, \varphi_2]f\|_Y \leq C\|f\|_X \|\varphi_1 - \varphi_2\|_X. \tag{13}$$

We compute the Gateaux derivative of F and find that

$$\partial_\varphi F[c, \varphi]f = \frac{3}{2}\varphi' f + \frac{3}{2}\varphi f' - [\mathscr{Q}, \mathscr{N}f]\varphi - [\mathscr{Q}, \mathscr{N}\varphi]f - \frac{1}{2}\mathscr{N}f - \frac{1}{2}f' - cf'.$$

Repeating the same estimates by making use of estimates (10) and Lemma 2.1 to deal with the Helmholtz operator $\mathscr{Q}$ we can easily check that (13) is indeed satisfied. Hence, we can conclude that the Gateaux derivative is continuous (indeed, it is Lipschitz) and then we can ensure the existence and continuity of the Fréchet derivative.

Next, we analyze the linearized operator at the trivial solution which is given by

$$\partial_\varphi F[c, 0]f(\xi) = -\frac{1}{2}\mathscr{N}f(\xi) - \frac{1}{2}f'(\xi) - cf'(\xi) := \mathsf{L}(f)(\xi) + \mathsf{K}(f)(\xi),$$

where

$$\mathsf{L}(f)(\xi) = -\frac{1}{2}f' - cf', \quad \text{and } \mathsf{K}(f)(\xi) = -\frac{1}{2}\mathcal{N}f.$$

The principal part of the operator $\mathsf{L}f : X \to Y$ is an isomorphism and hence has zero index. Moreover, using estimate (10), we infer that the operator $\mathsf{K}f : X \to Z$ is continuous and the embedding $Z \hookrightarrow Y$ is compact. Therefore, since the index of a Fredholm operator remains unchanged due to compact perturbations we conclude that $\partial_\varphi F[c,0]f$ is a Fredholm operator of zero index.

To conclude we characterize the kernel of the linear operator. For $f \in X$ we find that

$$\partial_\varphi F[c,0]f = \sum_{k=1}^{\infty} f_k \sin(kx)\left(-\frac{k}{2(1+k^2)} - \frac{k}{2} - ck\right).$$

Thus, for

$$c_k = -\frac{1}{2(1+k^2)} - \frac{1}{2}$$

we have that

$$\mathrm{Ker}(\partial_\varphi F[c,0]) = \mathrm{span}(\cos(kx))$$

and, recalling that the linearized operator is Fredholm operator of zero index,

$$Y/Img(\partial_\varphi F[c,0]) = \mathrm{span}(\sin(kx)).$$

The transversality condition is then satisfied because

$$\partial_c\partial_\varphi F[c_k,0]f = \sum_{k=1}^{\infty} f_k \sin(kx)(-k),$$

and, if $f \in \mathrm{Ker}(\partial_\varphi F[c,0])$, then

$$\partial_c\partial_\varphi F[c_k,0]f = -kf_k \sin(kx) \notin Img(\partial_\varphi F[c,0]).$$

3.3. Proof of Theorem 2

We have checked that the Crandall–Rabinowitz theorem can be applied in our Eq. (11). Fix $m \geq 1$. In order to prove Theorem 2, let us introduce the symmetry m in the spaces. For that, let us define

$$X_m := \left\{ f \in C^{1,\alpha}([0,2\pi]), \quad f(\xi) = \sum_{k\geq 1} f_k \cos(mk\xi) \text{ with norm } \|f\|_{X_m} = \|f\|_{C^{1,\alpha}} \right\},$$

$$Y_m := \left\{ f \in C^{0,\alpha}([0,2\pi]), \quad f(\xi) = \sum_{k\geq 1} f_k \sin(mk\xi) \text{ with norm } \|f\|_{Y_m} = \|f\|_{C^{0,\alpha}} \right\},$$

for any $m \geq 1$. The fact that the operator $F : \mathbb{R} \times X_m \to Y_m$ is well-defined and $\mathscr{C}^1(\mathbb{R} \times X_m \to Y_m)$ can be checked by repeating the computations of Section 3.2. However, we have to show that the m-fold symmetry property holds. More precisely, we have to proof that if $\varphi(\xi + \frac{2\pi}{m}) = \varphi(\xi)$ then

$$F[c,\varphi](\xi + \frac{2\pi}{m}) = F[c,\varphi](\xi).$$

Note that if φ has m-fold symmetry, then all the derivatives of φ also enjoy the same symmetry property. Moreover, recalling that $\mathcal{Q}$ is a convolution operator (6), the symmetry is also satisfied and thus $F[c,\varphi](\xi + \frac{2\pi}{m}) = F[c,\varphi](\xi)$ follows. The rest of the arguments can be argued similarly as in the previous Section 3.2. Thus, Crandall–Rabinowitz theorem can be applied obtaining Theorem 2.

4. Traveling wave solutions of the nonlocal wave equation

In this section the existence of traveling wave solutions of the unidirectional model is analyzed. As mentioned in the introduction, this will be made by using normal form theory, [18–20], and the results will be supported by numerical experiments of generation with the procedure described in Appendix. The experiments have the twofold goal of illustrating the theoretical results and suggesting additional properties of the emerging waves not specifically derived from the theory.

Note first, [7], that from the identity

$$[\mathscr{L}, \mathcal{N}]\, h = \mathscr{L}\,(h\mathcal{N}h) + \frac{1}{2}\partial_x\,(\mathcal{N}h)^2\,,$$

(5) can be written in the alternative form

$$h_t + \partial_x\left(\frac{3}{4}h^2 + \frac{1}{2}\mathcal{N}(h\mathcal{N}h) - \frac{1}{4}(\mathcal{N}h)^2 - \frac{1}{2}\mathcal{Q}h - \frac{h}{2}\right) = 0. \tag{14}$$

An additional property that will be used below is a formulation of (5) involving local terms: if

$$\mathscr{J} = \mathcal{Q}^{-1}, h = \mathscr{J}u, \tag{15}$$

then (14) can be formulated as

$$\mathscr{J}u_t + \partial_x\left(\frac{3}{4}(\mathscr{J}u)^2 + \frac{1}{2}\partial_x\mathscr{J}^{-1}\left((\mathscr{J}u)\partial_x u\right) - \frac{1}{4}(\partial_x u)^2 - \frac{1}{2}u - \frac{\mathscr{J}u}{2}\right) = 0. \tag{16}$$

For traveling wave solutions $h = h(x - c_s t)$ of (14), the profiles $h = h(X), X = x - c_s t$ must satisfy, from (14) and after one integration

$$-c_s h + \left(\frac{3}{4}h^2 + \frac{1}{2}\mathcal{N}(h\mathcal{N}h) - \frac{1}{4}(\mathcal{N}h)^2 - \frac{1}{2}\mathcal{Q}h - \frac{h}{2}\right) + g = 0, \tag{17}$$

with g constant. (Note that h is not necessarily localized.) In terms of the variable u, defined in (15), (17) yields

$$-c_s\mathscr{J}^2u + \left(\frac{3}{4}\mathscr{J}(\mathscr{J}u)^2 + \frac{1}{2}\partial_x\left((\mathscr{J}u)\partial_x u\right) - \frac{1}{4}\mathscr{J}(\partial_x u)^2 - \frac{1}{2}\mathscr{J}u - \frac{\mathscr{J}^2u}{2}\right) + g = 0, \tag{18}$$

which can be written as

$$\begin{aligned}\left(\frac{3}{2}\mathscr{J}u - \widetilde{c}_s\right)u'''' - \left(2\widetilde{c}_s + \frac{1}{2}\right)u'' + \left(\widetilde{c}_s + \frac{1}{2}\right)u \\ = \widetilde{f}(u,u',u'',u''') = f(u,u',u'',u''') + g \\ = \frac{1}{2}\left(\frac{3}{2}u^2 + \frac{7}{2}(u')^2 + uu'' - \frac{3}{2}(u'')^2 - 6u'u''' + 3(u''')^2\right) + g,\end{aligned} \tag{19}$$

where $\widetilde{c}_s = c_s + \frac{1}{2}$.

Eq. (18) can also be formulated as a first-order system for $Y = (y_1, y_2, y_3, y_4)^T = (u, u', u'', u''')^T$ as

$$\begin{aligned}\frac{dy_1}{dX} &= y_2,\\ \frac{dy_2}{dX} &= y_3,\\ \frac{dy_3}{dX} &= y_4,\\ \frac{dy_4}{dX} &= \frac{1}{\alpha(y_1,y_3,\widetilde{c}_s)}\left(g + F(Y)\right),\end{aligned} \tag{20}$$

where

$$\alpha(y_1,y_3,\widetilde{c}_s) = \frac{3}{2}(y_1 - y_3) - \widetilde{c}_s, \tag{21}$$

$$\begin{aligned}F(Y) = &\left(2\widetilde{c}_s + \frac{1}{2}\right)y_3 - \left(\widetilde{c}_s + \frac{1}{2}\right)y_1 \\ &+ \frac{1}{2}\left(\frac{3}{2}y_1^2 + \frac{7}{2}y_2^2 + y_1y_3 - \frac{3}{2}y_3^2 - 6y_2y_4 + 3y_4^2\right).\end{aligned} \tag{22}$$

The equivalence between (18) and (20)–(22) requires $\alpha \neq 0$. The case $\alpha = 0$ means that

$$\frac{3}{2}\mathscr{J}u - \widetilde{c}_s = 0 \Rightarrow h = \frac{2}{3}\widetilde{c}_s,$$

which is a constant solution of (14) with $g = (\widetilde{c}_s^2 + \widetilde{c}_s)/3$. Out of this, the transformation $dX = \alpha dZ$ leads to the nonsingular system, [29]

$$\begin{aligned}\frac{dy_1}{dZ} &= \alpha y_2,\\ \frac{dy_2}{dZ} &= \alpha y_3,\\ \frac{dy_3}{dZ} &= \alpha y_4,\\ \frac{dy_4}{dZ} &= g + F(Y),\end{aligned} \tag{23}$$

Note that the system (23) has the same phase dynamical behavior as system (20), except for the line $\alpha = \frac{3}{2}(y_1 - y_3) - \widetilde{c_s} = 0$, which is a line solution for (23). When discussing the equilibria of (23), we distinguish two cases:

(i) $\alpha = 0$. Then

$$y_1 = y_3 + \frac{2}{3}\left(c_s + \frac{1}{2}\right).$$

Furthermore, after some tedious algebra, the condition $g + F(Y) = 0$ can be written as

$$\frac{7}{2}x_1^2 + \frac{3}{7}x_2^2 + x_3^2 + 2(g - g_2(c_s)) = 0, \tag{24}$$

where

$$x_1 = y_2 - \frac{6}{7}y_4, \quad x_2 = y_4, \quad x_3 = y_3 + \frac{7}{3}\left(c_s + \frac{1}{2}\right), \tag{25}$$

and

$$g_2(c_s) := \frac{1}{3}\left(c_s + \frac{1}{2}\right) + \frac{52}{9}\left(c_s + \frac{1}{2}\right). \tag{26}$$

Note that:

- If $g > g_2(c_s)$, there are no points (x_1, x_2, x_3) satisfying (24).
- If $g = g_2(c_s)$, the only point satisfying (24) is $x_1 = x_2 = x_3 = 0$. Since the inverse of (25) is

$$y_2 = x_1 + \frac{6}{7}x_2, \quad y_4 = x_2, \quad y_3 = x_3 - \frac{7}{3}\left(c_s + \frac{1}{2}\right), \tag{27}$$

and

$$y_1 = y_3 + \frac{2}{3}\left(c_s + \frac{1}{2}\right) = x_3 - \frac{5}{3}\left(c_s + \frac{1}{2}\right), \tag{28}$$

then the origin is transformed into

$$y_1 = -\frac{5}{3}\left(c_s + \frac{1}{2}\right), y_2 = 0, y_3 = -\frac{7}{3}\left(c_s + \frac{1}{2}\right), y_4 = 0.$$

- If $g < g_2(c_s)$, then we have the equilibria (27), (28), where (x_1, x_2, x_3) are the points of the ellipsoid (24).

(ii) $\alpha \neq 0$. Then $y_2 = y_3 = y_4 = 0$ and the condition $g + F(Y) = 0$ reads

$$y_1^2 - \frac{4}{3}\left(c_s + 1\right) y_1 + \frac{4}{3}g = 0,$$

leading to the solutions

$$y_1 = y_\pm = \frac{2}{3}\left(\left(c_s + 1\right) \pm \sqrt{\left(c_s + 1\right)^2 - 3g}\right). \tag{29}$$

Then, the solutions (29) are real when

$$g \leq g_1(c_s) := \frac{1}{3}\left(c_s + 1\right)^2. \tag{30}$$

(Note that $g_1(c_s) < g_2(c_s)$ for all $c_s > 0$.) We may summarize the previous analysis as follows.

Proposition 4.1. *Let $c_s > 0$ and $g_1(c_s), g_2(c_s)$ be given respectively by (26) and (30). The following holds:*

(1) *If $g < g_1(c_s)$ then we have the equilibria*

$$\widetilde{Y} = (y_\pm, 0, 0, 0), \tag{31}$$

$$Y^* = \left(x_3 - \frac{5}{3}\left(c_s + \frac{1}{2}\right), x_1 + \frac{6}{7}x_2, x_3 - \frac{7}{3}\left(c_s + \frac{1}{2}\right), x_2\right), \tag{32}$$

where $y_\pm$ is given by (29) and (x_1, x_2, x_3) are the points of the ellipsoid (24).

(2) *If $g = g_1(c_s)$, then (32) holds and (31) becomes*

$$\widetilde{Y} = (y_1, 0, 0, 0), \quad y_1 = y_\pm = \frac{2}{3}\left(c_s + 1\right).$$

(3) *If $g_1(c_s) < g < g_2(c_s)$, then we just have the equilibria (32).*

(4) *If $g = g_2(c_s)$, then the equilibria (32) reduces to*

$$Y^* = \left(-\frac{5}{3}\left(c_s + \frac{1}{2}\right), 0, -\frac{7}{3}\left(c_s + \frac{1}{2}\right), 0\right),$$

corresponding to $x_1 = x_2 = x_3 = 0$.

(5) *If $g > g_2(c_s)$, then there are no equilibria.*

4.1. The case $g \leq g_1(c_s)$

For $c_s > 0$ fixed, the present paper is focused on the existence of traveling wave solutions of (14) or (16) around the equilibria (31) in the cases (1) and (2) of Proposition 4.1. They will emerge as homoclinic trajectories of a related reversible dynamical system and from the application of normal form theory, approaching y_+ (or y_-) when $t \to \pm\infty$. Note in particular that when $g = 0$ then

$$y_+ = \frac{1}{3}\left(c_s + 1\right), \quad y_- = 0,$$

and those orbits homoclinic to y_- at infinity are identified as solitary wave solutions, with the meaning of localized traveling wave solutions. In addition, periodic orbits of the dynamical system are identified as periodic traveling wave (PTW) solutions.

To this end, our approach will first look for a reduction of (19) to the case $g = 0$. Let $y_\pm$ denote any of the equilibria (29). Note that if u is a solution of (19), then $\widetilde{u} = u - y_\pm$ satisfies

$$\left(\frac{3}{2}\mathscr{f}\widetilde{u} + \frac{3y_\pm - 1}{2} - c_s\right)\widetilde{u}''' + \left(2c_s + \frac{3 - 5y_\pm}{2}\right)\widetilde{u}' + \left(-c_s + \frac{3y_\pm - 2}{2}\right)\widetilde{u} = f(\widetilde{u}, \widetilde{u}', \widetilde{u}'', \widetilde{u}''')$$
$$= \frac{1}{2}\left(-\frac{3}{2}\widetilde{u}^2 + \frac{5}{2}(\widetilde{u}')^2 + 5\widetilde{u}\widetilde{u}'' - \frac{9}{2}(\widetilde{u}'')^2 - 6\widetilde{u}'\widetilde{u}''' + 3(\widetilde{u}''')^2\right), \tag{33}$$

As before, (33) can be written as a first-order system for $U = (U_1, U_2, U_3, U_4)^T = (\widetilde{u}, \widetilde{u}', \widetilde{u}'', \widetilde{u}''')^T$ as

$$\frac{dU}{dZ} = L(c_s, y_\pm)U + G(U), \tag{34}$$

where

$$L = L(c_s, y_\pm) = \begin{pmatrix} 0 & \frac{3y_\pm - 1}{2} - c_s & 0 & 0 \\ 0 & 0 & \frac{3y_\pm - 1}{2} - c_s & 0 \\ 0 & 0 & 0 & \frac{3y_\pm - 1}{2} - c_s \\ c_s + \frac{2 - 3y_\pm}{2} & 0 & -(2c_s + \frac{3 - 5y_\pm}{2}) & 0 \end{pmatrix},$$

$$G(U) = \begin{pmatrix} \frac{3}{2}U_2(U_1 - U_3) \\ \frac{3}{2}U_3(U_1 - U_3) \\ \frac{3}{2}U_4(U_1 - U_3) \\ \widetilde{F}(U) \end{pmatrix},$$

$$\widetilde{F}(U) = -\left(\frac{9}{4}U_3^2 - \frac{5}{2}U_1U_3\right) - \frac{3}{4}U_1^2 + \frac{5}{4}U_2^2 - 3U_2U_4 + \frac{3}{2}U_4^2.$$

The structure of solutions of (14) or (16) around $y_\pm$ can be analyzed from that of solutions of (34) around $U = 0$. Since $G(0) = G'(0) = 0$, then, if we first linearize, the characteristic polynomial of L is of the form $z^4 - bz^2 + a$, where

$$a = a_\pm = -\beta_\pm\alpha_\pm^3, \quad b = b_\pm = -\alpha_\pm\gamma_\pm,$$
$$\alpha_\pm = \frac{3y_\pm - 1}{2} - c_s, \quad \beta_\pm = c_s + \frac{2 - 3y_\pm}{2}, \quad \gamma_\pm = 2c_s + \frac{3 - 5y_\pm}{2}, \tag{35}$$

We note that (34) is reversible with respect to the transformation

$$S : (U_1, U_2, U_3, U_4) \mapsto (U_1, -U_2, U_3, -U_4), \tag{36}$$

in the sense that, [20]

$$SLU = -LSU, \quad SG(U) = -G(SU).$$

This implies that the linear dynamics around $U = 0$ follows Fig. 1, [18], in the (b, a) plane. Four regions of different dynamics are determined from the four curves

$$C_0 = \{(b, a)/a = 0, b > 0\},$$
$$C_1 = \{(b, a)/a = 0, b < 0\},$$
$$C_2 = \{(b, a)/a > 0, b = -2\sqrt{a}\},$$
$$C_3 = \{(b, a)/a > 0, b = 2\sqrt{a}\}. \tag{37}$$

On the curve C_0 there are two zero eigenvalues and two real $\pm\sqrt{b}$; on C_1 there are two zero eigenvalues and two imaginary $\pm i\sqrt{|b|}$; on

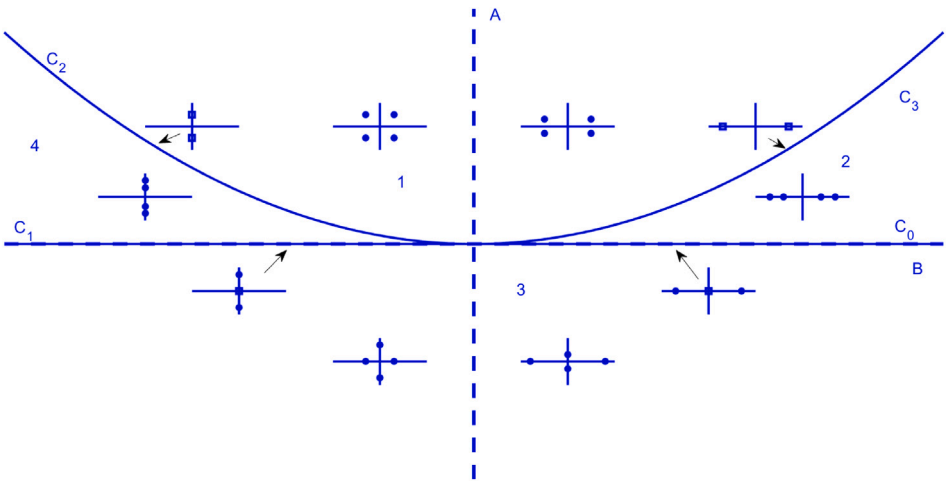

Fig. 1. Linearization at the origin of (34) (cf. [18, Figure 1]): Regions 1 to 4 in the (b,a)-plane, delimited by the bifurcation curves C_0 to C_3 given by (37), and schematic representation of the position in the complex plane of the eigenvalues of L for each curve and region. (Dot: simple root, square: double root.).

C_2 there is a double complex conjugate pair of imaginary eigenvalues $\pm i\sqrt{|b|/2}$, and on C_3 there are two double real eigenvalues $\pm\sqrt{b/2}$, symmetric with respect to the imaginary axis. The spectrum of L in the regions delimited by the four curves is represented schematically in Fig. 1.

The application of the normal form theory to systems of the form (34), cf. e. g. [20], aims at finding a change of variables to transform, near the equilibrium, the system into some fixed-order approximation from which the dynamics of the original one can be analyzed in a simpler way. The use of normal forms to study the existence of traveling waves as homoclinic trajectories typically involves bifurcation parameters as well as symmetries and reversible transformations, which determine the construction of the corresponding normal form and the emergence of different types of traveling waves, cf. [18] and references therein.

For reversible systems like (34), with $\mu = \mu(c_s)$ some bifurcation parameter (somehow related to the speed c_s), the normal form theorem, [20,30], states, for any integer $m \geq 2$, the existence of neighborhoods V_1 of $U = 0$ and V_2 of $\mu = 0$ such that for any $\mu \in V_2$ one can find a polynomial $\Phi(\mu,\cdot) : \mathbb{R}^4 \to \mathbb{R}^4$ of degree m satisfying:

(i) The coefficients of Φ are smooth functions of μ and

$$\Phi(0,0) = 0, \quad \partial_U \Phi(0,0) = 0.$$

(ii) For $V \in V_1$, the change of variable

$$U = V + \Phi(\mu, V),$$

transforms (34) into the normal form

$$V' = LV + N(\mu, V) + \rho(\mu, V),$$

with the following properties:

(a) For any $\mu \in V_2$, $N(\mu,\cdot) : \mathbb{R}^4 \to \mathbb{R}^4$ is a polynomial of degree m, with coefficients which are smooth functions of μ and $N(0,0) = \partial_V N(0,0) = 0$.

(b) The equality

$$N(\mu, e^{tL^*}V) = e^{tL^*}N(\mu, V),$$

holds for all $(t,V) \in \mathbb{R}\times\mathbb{R}^4$ and $\mu \in V_2$, and where L^* denotes the adjoint of L. This is shown to be equivalent, [20], to

$$\partial_V N(\mu,V)L^*V = L^*N(\mu,V), \quad V \in \mathbb{R}^4, \mu \in V_2.$$

(c) The function ρ is smooth in $(\mu,V) \in V_2 \times V_1$ such that

$$\rho(\mu,V) = o(\|V\|^m),$$

for all $\mu \in V_2$ and where $\|\cdot\|$ denotes the Euclidean norm in $\mathbb{R}^4$.

(d) The polynomials $\Phi(\mu,\cdot), N(\mu,\cdot)$ satisfy, for all $\mu \in V_2$

$$S\Phi(\mu,V) = \Phi(\mu,SV), \quad SN(\mu,V) = -N(\mu,SV), \quad V \in \mathbb{R}^4,$$

where S is given in (36).

The application of the normal form theory to (34) also involves the analysis of the system from a center manifold reduction. This will be done here by using the approach developed in [31,32] (see also [33]), by determining a normal form of an equivalent system to (34) and studying its principal part (linear and quadratic) near the bifurcation curves (37) with respect to some bifurcation parameter. Then this analysis, that concerns the reduction to the case $g = 0$ given by (33), will be used to discuss the existence of traveling waves of (14) and (16) homoclinic to the equilibria (31) at infinity, in terms if g and illustrating the results with experiments of numerical generation of the traveling wave profiles from the approximation to solutions of (33). To this last point, an iterative numerical procedure described in Appendix is implemented.

4.2. Some preliminary lemmas

The analysis below will require some previous results concerning the coefficients (35) and new relevant values of the constant g. We note first that when $g \leq g_1(c_s)$ then $0 \leq y_- \leq y_+$. Furthermore, it is not hard to prove the following result.

Lemma 4.2. *Let $c_s > 0$ and assume that $g \leq g_1(c_s)$. We define*

$$g_1^*(c_s) := g_1(c_s) - \frac{1}{75}\left(c_s - \frac{1}{2}\right)^2, \quad g_1^{**}(c_s) := g_1(c_s) - \frac{1}{12}. \tag{38}$$

Then it holds that:

(1) $\alpha_+ > 0, \beta_+ \leq 0, \beta_- \geq 0$.
(2) $\alpha_- \geq 0 \Leftrightarrow g \geq g_1^{**}(c_s)$.
(3) $\gamma_+ > 0 \Leftrightarrow c_s > \frac{1}{2}$ *and* $g > g_1^*(c_s)$.
(4) $\gamma_- > 0 \Leftrightarrow c_s \geq \frac{1}{2}$ *or* $g < g_1^*(c_s)$ *when* $c_s < \frac{1}{2}$.

In addition, for each case y_+, y_-, we will need to identify the position of the roots of characteristic polynomial of L in the (b,a) plane from the sign of the coefficients $a_\pm, b_\pm$ and $\Delta_\pm = b_\pm^2 - 4a_\pm$. After some computations, we observe that

$$\Delta_\pm = \alpha_\pm^2 S_\pm,$$
$$S_\pm = \gamma_\pm^2 + 4\alpha_\pm\beta_\pm = -\frac{11}{9}(\beta_\pm - \delta_+)(\beta_\pm - \delta_-),$$

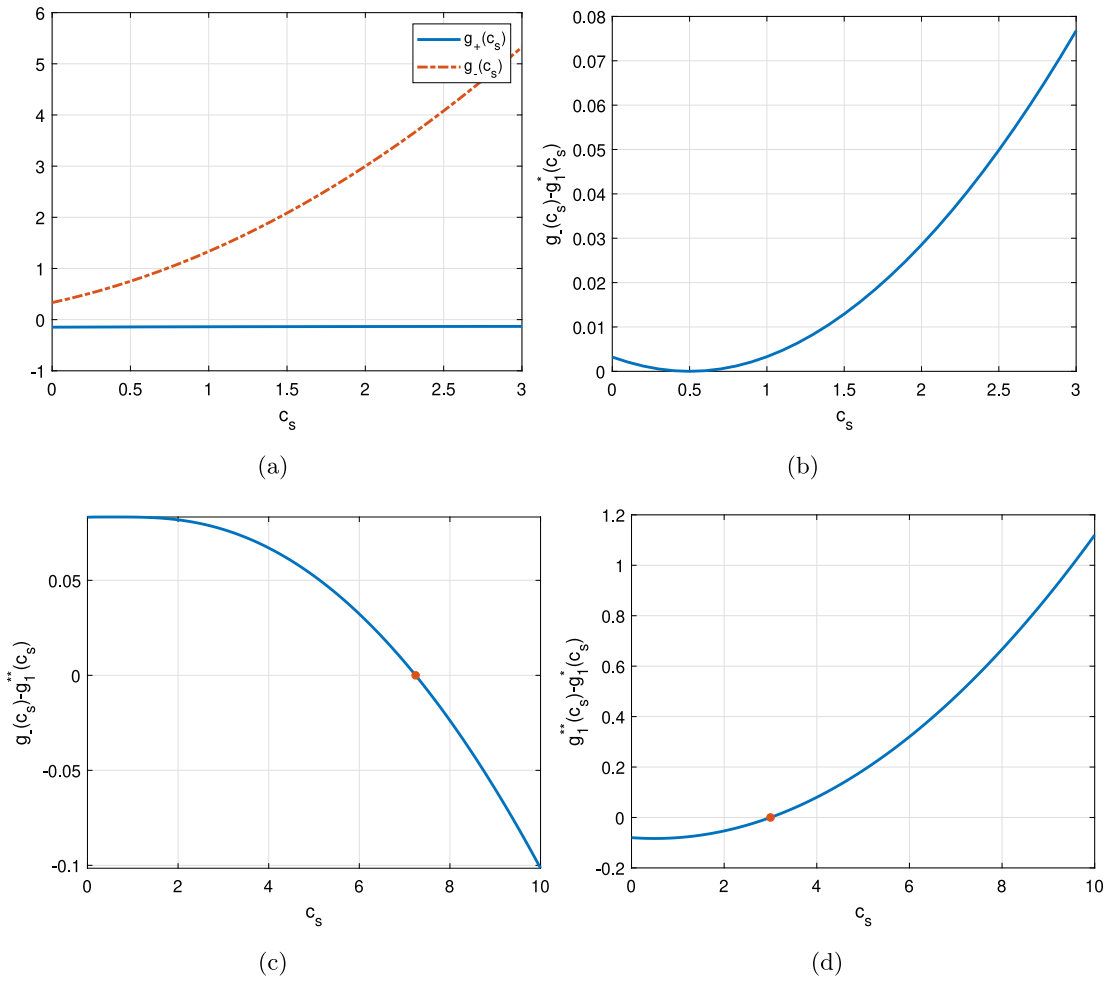

Fig. 2. Illustration of Lemma 4.4. (a), (b) Case (1); (c) Case (2), where the remarked dot corresponds to $c_s = 3(1+\sqrt{2})$; (d) Case (c), where the remarked dot corresponds to $c_s = 3$.

$$\delta_\pm = \frac{1}{22}\left((10c_s+13) \pm \sqrt{(10c_s+13)^2 + 44\left(c_s - \frac{1}{2}\right)^2}\right),$$

with $\delta_- < 0 < \delta_+$ for $c_s > 0$. This leads to the following properties:

Lemma 4.3. *Let $c_s > 0$ and assume that $g \le g_1(c_s)$. We define*

$$g_-(c_s) := g_1(c_s) - \frac{1}{3}\delta_-^2, \quad g_+(c_s) := g_1(c_s) - \frac{1}{3}\delta_+^2. \tag{39}$$

Then:

(i) $\Delta_+ > 0 \Leftrightarrow g > g_-(c_s)$.
(ii) *If $g_1^{**}(c_s) < g < g_1(c_s)$ then $\Delta_- > 0$. When $g < g_1^{**}(c_s)$ then*

$$\Delta_- > 0 \Leftrightarrow g > g_+(c_s).$$

A final result compares the limiting values of g appearing above and in Lemma 4.2 and it is illustrated in Fig. 2.

Lemma 4.4. *Let $c_s > 0$ and assume that $g \le g_1(c_s)$.*

(1) $g_+(c_s) < 0 < g_-(c_s)$ *and* $g_1^*(c_s), g_1^{**}(c_s) > 0$.
(2) $g_1^*(c_s) < g_-(c_s)$ *and* $g_1^{**}(c_s) \le g_-(c_s) \Leftrightarrow c_s \le 3(1+\sqrt{2})$.
(3) $g_1^*(c_s) \le g_1^{**}(c_s) \Leftrightarrow c_s \ge 3$,

where $g_1^*(c_s), g_1^{**}(c_s)$ and $g_+(c_s), g_-(c_s)$ are given by (38) and (39), respectively.

5. Existence of non-periodic traveling wave solutions

5.1. Normal forms

In what follows, we will assume $g \neq g^{**}(c_s)$ (so that $\alpha_- \neq 0$). In order to apply the theory of normal forms to (34), we first make the change of variable $dY = \alpha_\pm dZ$, which transforms the system to the equivalent form

$$\frac{dU}{dY} = \widetilde{L}U + \widetilde{G}(U), \tag{40}$$

where

$$\widetilde{L} = \begin{pmatrix} 0 & 1 & 0 & 0 \\ 0 & 0 & 1 & 0 \\ 0 & 0 & 0 & 1 \\ -\widetilde{a}_\pm(c_s) & 0 & \widetilde{b}_\pm(c_s) & 0 \end{pmatrix}, \tag{41}$$

$$\widetilde{G}(U) = \frac{1}{\alpha_\pm}G(U), \quad \widetilde{a}_\pm(c_s) = -\frac{\beta_\pm}{\alpha_\pm}, \quad \widetilde{b}_\pm(c_s) = -\frac{\gamma_\pm}{\alpha_\pm}. \tag{42}$$

Note that the characteristic polynomial of (41) is $p_{\widetilde{L}}(z) = z^4 - \widetilde{b}_\pm z^2 + \widetilde{a}_\pm$, and since

$$\widetilde{\Delta}_\pm := \widetilde{b}_\pm^2 - 4\widetilde{a}_\pm = \frac{S_\pm}{\alpha_\pm^4},$$

then the regions and curves of Fig. 1 in the (b,a)- and the $(\widetilde{b},\widetilde{a})$-plane are similar.

The matrix (41) can also be decomposed as $\widetilde{L} = L_0 + L_1$, where

$$L_0 = \begin{pmatrix} 0 & 1 & 0 & 0 \\ 0 & 0 & 1 & 0 \\ 0 & 0 & 0 & 1 \\ 0 & 0 & 0 & 0 \end{pmatrix}, \quad L_1 = \begin{pmatrix} 0 & 0 & 0 & 0 \\ 0 & 0 & 0 & 0 \\ 0 & 0 & 0 & 0 \\ -\widetilde{a}_{\pm}(c_s) & 0 & \widetilde{b}_{\pm}(c_s) & 0 \end{pmatrix}. \tag{43}$$

The computation of a reversible normal form for (40) can be made following the approach in [31] and using the arguments of [32] in order to include the matrix L_1 in (43) in the construction. This consists of deriving an equivalent reversible system

$$\frac{dU}{dY} = (L_0 + R_1)U + \widetilde{G}(U), \tag{44}$$

with R_1 satisfying

$$R_1 L_0^* = L_0^* R_1, \quad SR_1 = -R_1 S,$$

where L_0^* denotes the adjoint of L_0 and S is given by (36). Explicitly, [32]

$$R_1 = \begin{pmatrix} 0 & 1 & 0 & 0 \\ \mu_1 & 0 & 1 & 0 \\ 0 & \mu_1 & 0 & 1 \\ \mu_2 & 0 & \mu_1 & 0 \end{pmatrix}, \quad \mu_1 = \frac{\widetilde{b}_{\pm}}{3}, \quad \mu_2 = \mu_1^2 - \widetilde{a}_{\pm}. \tag{45}$$

After that, the computation of a normal form for (44), from the approach in [31], leads to the system

$$\begin{aligned} \frac{dU}{dY} &= L_0 U + P_4(U_1, V_2, V_4)\begin{pmatrix} 0 \\ 0 \\ 0 \\ 1 \end{pmatrix} + P_2(U_1, V_2, V_4)\begin{pmatrix} 0 \\ U_1 \\ U_2 \\ U_3 \end{pmatrix} \\ &+ P_0(V_2, V_4)\begin{pmatrix} 0 \\ V_2 \\ W_2 \\ X_2 \end{pmatrix} + P_1(U_1, V_2, V_4)\begin{pmatrix} V_3 \\ W_3 \\ X_3 \\ Y_3 \end{pmatrix} \\ &+ P_3(U_1, V_2, V_4)\begin{pmatrix} 0 \\ 0 \\ V_3 \\ W_3 \end{pmatrix}, \end{aligned} \tag{46}$$

where

$$\begin{aligned} &V_2 = U_2^2 - 2U_1U_3, \quad V_3 = U_2^3 - 3U_1U_2U_3 + 3U_1^2U_4, \\ &V_4 = 3U_2^2U_3^2 - 6U_2^3U_4 - 8U_1U_3^3 + 18U_1U_2U_3U_4 - 9U_1^2U_4^2, \\ &W_2 = -3U_1U_4 + U_2U_3, \quad W_3 = 3U_1U_2U_4 - 4U_1U_3^2 + U_2^2U_3, \\ &X_2 = -3U_2U_4 + 2U_3^2, \quad X_3 = -3U_1U_3U_4 + 3U_2^2U_1 - U_2U_3^2, \\ &Y_3 = 3U_2U_3U_4 - \frac{4}{3}U_3^3 - 3U_1U_4^2, \end{aligned}$$

and $P_j, j = 0, 1, 2, 3, 4$, are polynomials in their arguments. In the sequel the principal part (linear and quadratic) of the normal form will be used. Due to the form of the right-hand side of (46), observe that the contribution of P_1 and P_3 is of order three while

$$\begin{aligned} P_4(U_1, V_2, V_4) &= \mu_2 U_1 + \nu_1 U_1^2 + \nu_2 V_2 + O(\|U\|^3), \\ P_2(U_1, V_2, V_4) &= \mu_1 + \nu_3 U_1 + (\|U\|^2), \\ P_0(V_2, V_4) &= \nu_4 + O(\|U\|^2), \end{aligned}$$

for some constants $\nu_j, j = 1, 2, 3, 4$, and where μ_1, μ_2 are given by (45). Note that the linearization of (46) at $U = 0$ leads to the linearized system of (44), which has the same characteristic polynomial as $\widetilde{L}$ in (41), so the spectrum of the linear part is preserved. From the relations in (45), the bifurcation curves (37) can be written in the (μ_1, μ_2)-plane as

$$\begin{aligned} C_0 &= \{(\mu_1, \mu_2) | \mu_1 > 0, \mu_2 = \mu_1^2\}, \\ C_1 &= \{(\mu_1, \mu_2) | \mu_1 < 0, \mu_2 = \mu_1^2\}, \\ C_2 &= \{(\mu_1, \mu_2) | \mu_1 < 0, \mu_2 = -\frac{5}{4}\mu_1^2\}, \\ C_3 &= \{(\mu_1, \mu_2) | \mu_1 > 0, \mu_2 = -\frac{5}{4}\mu_1^2\}. \end{aligned} \tag{47}$$

(Cf. Figure 1 of [31].) Following [31,32], now we describe the principal part of the normal form (46) near the curves (37). The emergence of homoclinic orbits will be related to the existence of traveling wave solutions of (14) in Section 5.3.

5.2. Principal part of normal forms near the curves (37)

5.2.1. Normal form near C_0

If we take $\mu = -\widetilde{a}_{\pm}$ as bifurcation parameter, then $\mu_2 = \mu_1 + \mu$ and from (47)C_0 can be described by the conditions $\mu = 0, \mu_1 > 0$. Recall that in C_0 the spectrum of $L_0 + R_1$ contains a double zero eigenvalue and two real eigenvalues $\pm\sqrt{3\mu_1}$. In [31,32], a basis of $\mathrm{Ker}(L_0 + R_1)^2$ is computed as

$$\xi_0 = (1, 0, -\mu_1, 0)^T, \quad \xi_1 = (0, 1, 0, -2\mu_1)^T, \tag{48}$$

satisfying $(L_0 + R_1)\xi_1 = \xi_0$ and $S\xi_0 = \xi_0, S\xi_1 = -\xi_1$. The Center Manifold Theorem applies to study the dynamics near C_0 on the two-dimensional center manifold. After a suitable change of variables

$$U = A\xi_0 + B\xi_1 + \Phi(\mu, A, B),$$

with some Φ, the corresponding principal part of the normal form is, cf. [32],

$$\begin{aligned} \frac{dA}{dY} &= B, \\ \frac{dB}{dY} &= -\frac{\mu}{3\mu_1}A + \widetilde{c}(\mu_1)A^2, \end{aligned} \tag{49}$$

where

$$\widetilde{c}(\mu_1) = \frac{P(\mu_1)}{3\alpha_{\pm}\mu_1}, \quad P(\mu_1) = \frac{3}{4} + \frac{5}{2}\mu_1 + \frac{5}{4}\mu_1^2 - \mu_1^3. \tag{50}$$

(The system can be reformulated to avoid the singularity as $\mu_1 \to 0$, cf. [31].) If $\mu < 0$ (that is, $\widetilde{a}_{\pm} > 0$, region 2 of Fig. 1) then (49) admits a homoclinic to zero solution in the form of a KdV-type solitary wave, whose persistence for the original system as traveling wave solution homoclinic to $y_{\pm}$ at infinity can be followed from the arguments in e. g. [18,19]. The characterization of the wave as of elevation or of depression is given by the sign of (50), being of elevation if $\widetilde{c}(\mu_1) < 0$ and of depression if $\widetilde{c}(\mu_1) > 0$. Note that, from Lemma 4.2 and the condition $\mu < 0$ imply that $\alpha_+\mu_1 > 0$ while $\alpha_-\mu_1 > 0$. On the other hand, the polynomial $P(\mu_1), \mu_1 > 0$ has only one real zero μ_1^*, being positive when $\mu < \mu_1^*$ and negative when $\mu > \mu_1^*$. Therefore:

- For $\mu_1 < \mu_1^*$, the traveling wave profile homoclinic to y_+ is of depression and the one homoclinic to y_- is of elevation.
- For $\mu_1 > \mu_1^*$, the traveling wave profile homoclinic to y_+ is of elevation and the one homoclinic to y_- is of depression.

On the other hand, when $\mu > 0$ is small (region 3, right, of Fig. 1), the normal form (49) admits periodic solutions, which correspond to periodic traveling wave solutions of (14).

5.2.2. Normal form near C_1

Using the previous bifurcation parameter and (47), now C_1 is characterized as $\mu = 0, \mu_1 < 0$. In C_1 the spectrum of $L_0 + R_1$ consists of a double zero eigenvalue and two imaginary eigenvalues $\pm i\sqrt{-3\mu_1}$. The eigenvectors $\zeta_0, \overline{\zeta_0}$, where, [31]

$$\zeta_0 = (1, i\sqrt{-3\mu_1}, 2\mu_1, i\mu_1\sqrt{-3\mu_1})^T,$$

along with ξ_0, ξ_1 defined by (48), form a basis of $\mathbb{C}^4$. When $\mu > 0$ (that is, $\widetilde{a}_{\pm} < 0$, region 3, left, of Fig. 1) the double zero eigenvalue changes to two real eigenvalues. After a change of variables

$$U = A\xi_0 + B\xi_1 + C\zeta_0 + \overline{C\zeta_0} + \Phi(\mu, A, B, C, \overline{C}),$$

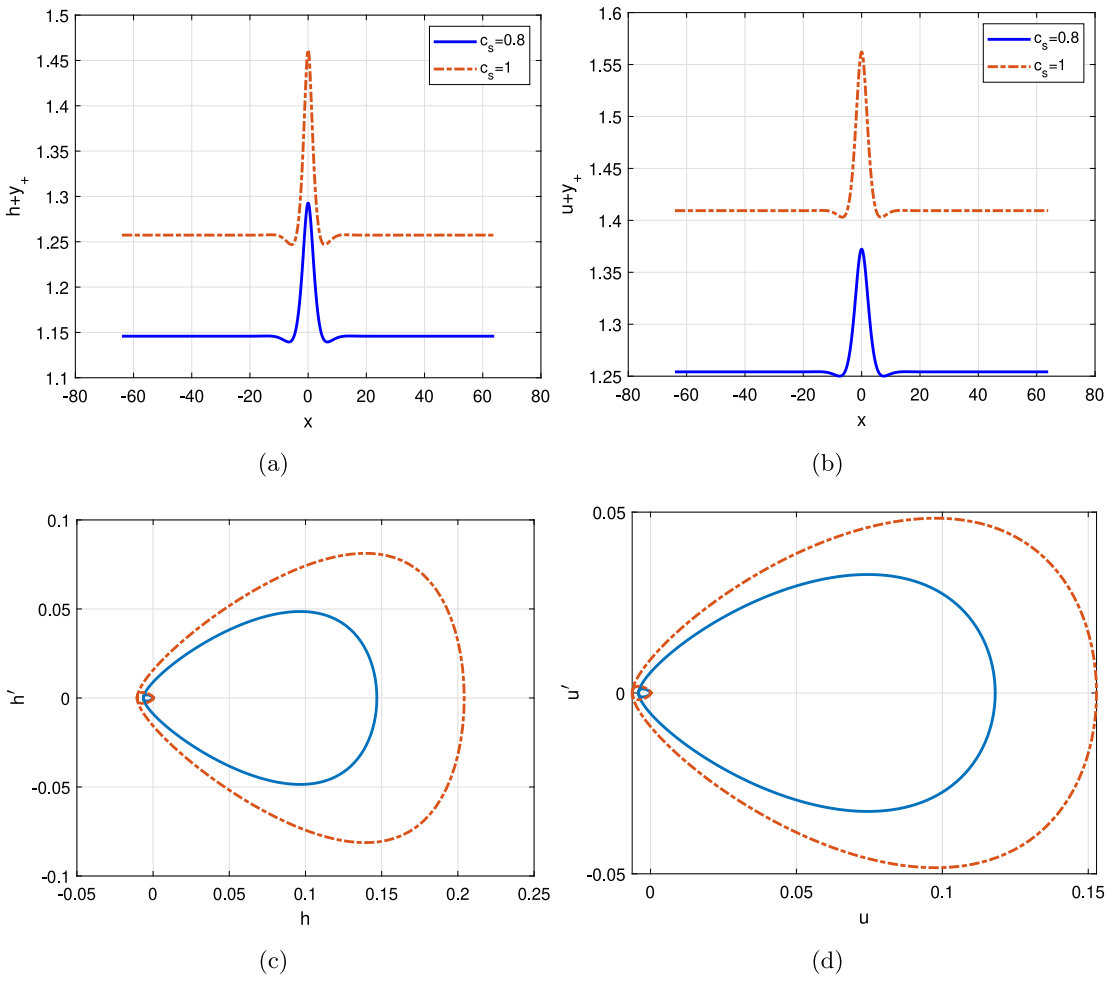

Fig. 3. Approximations to traveling wave solutions of (17) for two values of c_s. Case $g = g_1^*(c_s) - 0.001$. (a) $\widetilde{h} + y_+$ profile; (b) $\widetilde{u} + y_+$ profile; (c) $\widetilde{h}$ phase plot; (d) $\widetilde{u}$ phase plot. Region 1 (right) of Fig. 1.

and from the normal form given in [19,31], the construction made in [32] for quadratic nonlinearities, can be used to obtain the system

$$\begin{aligned}
\frac{dA}{dY} &= B,\\
\frac{dB}{dY} &= a_* A + b_* A^2 + c_* |C|^2,\\
\frac{dC}{dY} &= id_0 C + id_1 a_* C + id_2 AC,
\end{aligned} \tag{51}$$

where

$$a_* = -\frac{\mu}{3\mu_1}, \quad b_* = \widetilde{c}(\mu_1),$$
$$c_* = \frac{Q(\mu_1)}{3\alpha_\pm \mu_1}, \quad Q(\mu_1) = \frac{3}{2} - \frac{5}{2}\mu_1 + 6\mu_1^2 - 3\mu_1^3,$$
$$d_0 = \sqrt{-3\mu_1}, \quad d_1 = -\frac{d_0}{6\mu_1},$$

while d_2 is obtained from the relations

$$\begin{aligned}
b_1 &= id_2 - \frac{2}{\alpha_\pm}\left(\frac{3}{4}(1+\mu_1)i\sqrt{-3\mu_1}\right),\\
b_2 &= -d_2\sqrt{-3\mu_1} - \frac{2}{\alpha_\pm}\left(\frac{3}{4}\mu_1 + \frac{9}{4}\mu_1^2\right),\\
b_3 &= 2id_2\mu_1 - \frac{2}{\alpha_\pm}\left(\frac{3}{4}i\mu_1\sqrt{-3\mu_1}(1+\mu_1)\right),\\
b_4 &= -d_2\mu_1\sqrt{-3\mu_1} - \frac{2}{\alpha_\pm}\left(-\frac{3}{4} + \frac{5}{4}\mu_1 - \frac{9}{2}\mu_1^3\right),
\end{aligned}$$

and

$$b_4 + \frac{\mu_1}{2}\left(b_2 - \frac{i\mu_1}{\sqrt{-3\mu_1}}b_1\right) - \frac{3}{2}\frac{i\mu_1}{\sqrt{-3\mu_1}}\left(b_3 - \frac{i\sqrt{-3\mu_1}}{2}\left(b_2 - \frac{i\mu_1}{\sqrt{-3\mu_1}}b_1\right)\right) = 0.$$

System (51) admits orbits which are homoclinic to periodic orbits as $|Y| \to \infty$, and that may have exponentially small amplitude, [34]. They lead to the so-called generalized solitary waves, (cf. [23] and references therein), in contrast with the classical solitary waves, which are localized and correspond to homoclinic to zero orbits (like those near C_0, analyzed above). In some cases, [35], these orbits may contain embedded solitons, on curves where the oscillatory ripples vanish and a classical solitary wave emerges.

Note that in the case of y_+ and from Lemma 4.2, it is not hard to see that region 3 of Fig. 1 is not possible, preventing the existence of generalized traveling waves around that equilibria. However, region 3, left, is possible in the case of y_-; the generation of a generalized traveling is illustrated in Section 5.3. The numerical experiments also suggest some open questions on the persistence of these waves, [18,32].

When $\mu < 0$ (that is, $\widetilde{a}_\pm > 0$, region 4 of Fig. 1), the double zero eigenvalue splits into two imaginary eigenvalues and the normal form theory predicts the formation of periodic traveling wave solutions of (14) in the form of periodic orbits of (51).

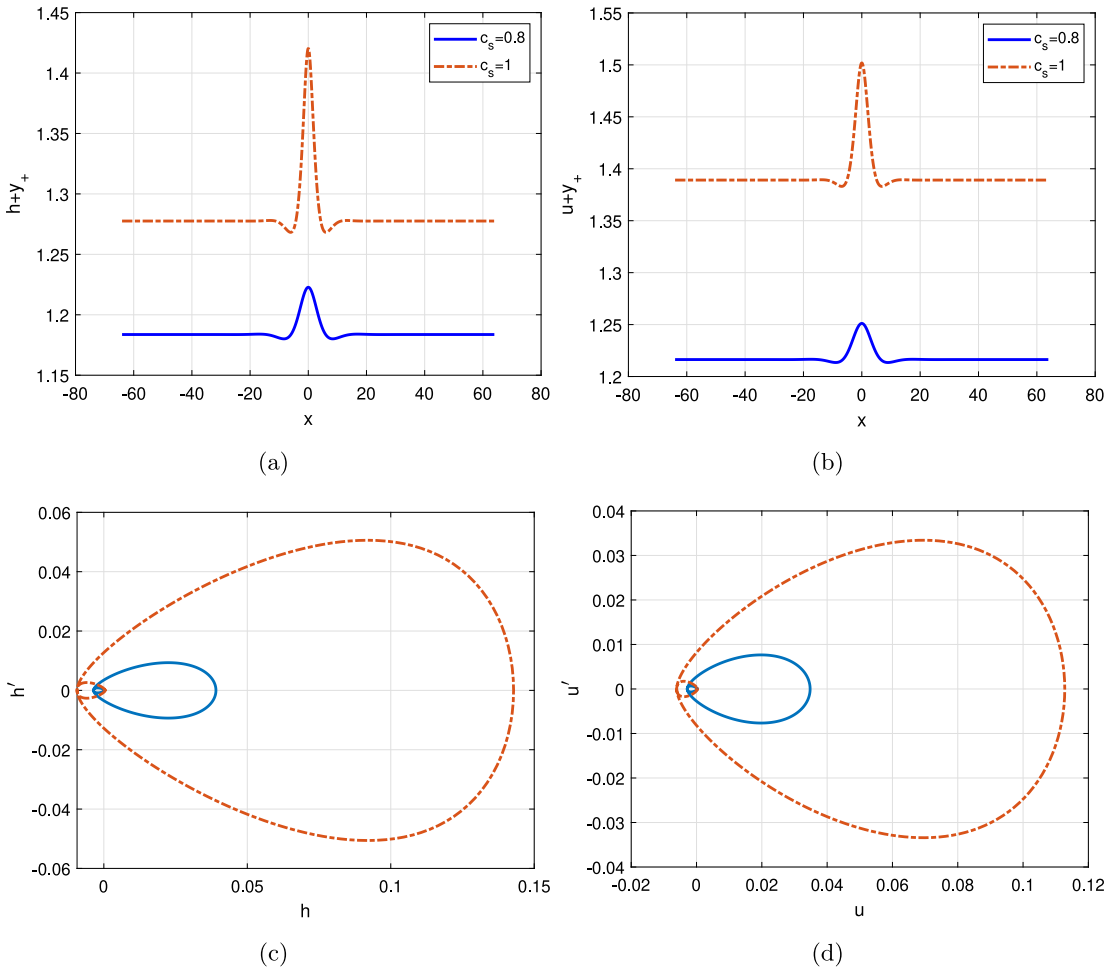

Fig. 4. Approximations to traveling wave solutions of (17) for two values of c_s. Case $g = g_1^*(c_s) + 0.001$. (a) $\widetilde{h} + y_+$ profile; (b) $\widetilde{u} + y_+$ profile; (c) $\widetilde{h}$ phase plot; (d) $\widetilde{u}$ phase plot. Region 1 (left) of Fig. 1.

5.2.3. Normal form near C_2

According to (47), C_2 can be characterized as $\mu = 0$ for a bifurcation parameter μ such that

$$\mu_2 = -\frac{5}{4}\mu_1^2 - \mu, \quad \mu_1 < 0.$$

The spectrum of $L_0 + R_1$ in C_2 has two double imaginary eigenvalues $\pm i q_\pm, q_\pm = \sqrt{-3\mu_1/2}$, and a basis of $\mathbb{C}^4$ can be constructed with the eigenvector $\zeta_0, \overline{\zeta_0}$ and the generalized eigenvectors $\zeta_1, \overline{\zeta_1}$, where, [31]

$$\zeta_0 = (1, iq_\pm, \frac{\mu_1}{2}, -\mu_1\frac{iq_\pm}{2})^T, \quad \zeta_1 = (0, 1, 2iq_\pm, \frac{5}{2}\mu_1)^T.$$

They can be used to make a change of variables of the form, [18,31,36,37]

$$U = A\zeta_0 + B\zeta_1 + \overline{A\zeta_0} + \overline{B\zeta_1} + \Phi(\mu, A, B, \overline{A}, \overline{B}),$$

leading to a normal form

$$\begin{aligned}
\frac{dA}{dY} &= iq_\pm A + B - \frac{i\mu A}{6\mu_1\sqrt{-6\mu_1}} + iAP_1(|A|^2, A\overline{B} - B\overline{A}),\\
\frac{dB}{dY} &= iq_\pm B - \frac{i\mu B}{6\mu_1\sqrt{-6\mu_1}} + iBP_1(|A|^2, A\overline{B} - B\overline{A})\\
&\quad - \frac{\mu}{6\mu_1}A + AQ_1(|A|^2, A\overline{B} - B\overline{A}),
\end{aligned} \tag{52}$$

where P_1, Q_1 are real polynomials of degree at least one in their arguments. The approaches in [37,38] apply to show the existence and persistence of orbits homoclinic to zero when $\mu > 0$ is small (region 1, left, of Fig. 1); the way how the orbits approach the origin is oscillatory, in contrast with the homoclinic trajectories close to C_0, which tend to the origin in a monotone way. This implies that the corresponding solitary wave solutions of (33), or traveling wave solutions of (14) homoclinic to $y_\pm$ at infinity, have a non-monotone decay. They are illustrated in Section 5.3; the character of the wave as of elevation or depression type seems to follow the same rules as those derived for the waves emerged near C_0.

When $\mu < 0$ (region 4, close to C_2, of Fig. 1), the spectrum consists of four imaginary eigenvalues and no homoclinic orbits are known to exists in general, [32], The numerical experiments in Section 5.3 suggest the existence of periodic traveling wave solutions, as periodic orbits of (52).

Finally, we note that from Lemmas 4.2–4.4, regions 1, left, and 4 are not possible in the dynamics around y_-.

5.2.4. Normal form near C_3

From the previous bifurcation parameter μ, with $\mu_1 > 0$, the spectrum of $L_0 + R_1$ in $C_3(\mu = 0)$ has two double real eigenvalues $\pm\sqrt{3\mu_1/2}$. In region 1, right, of Fig. 1 ($\mu > 0$ small), the eigenvalues split into two complex, simple, conjugate pairs and in region 2 ($\mu < 0$ small) they become four real eigenvalues. Then near C_3 the equilibrium $U = 0$ remains hyperbolic (either saddle-focus or saddle) and no small-amplitude bifurcation holds. When crossing from region 2 to region 1, different types of homoclinic orbits may be generated, in the form of multimodal homoclinic orbits (corresponding to multipulses), as well as classical solitary waves and periodic traveling waves, [18,22,37,39].

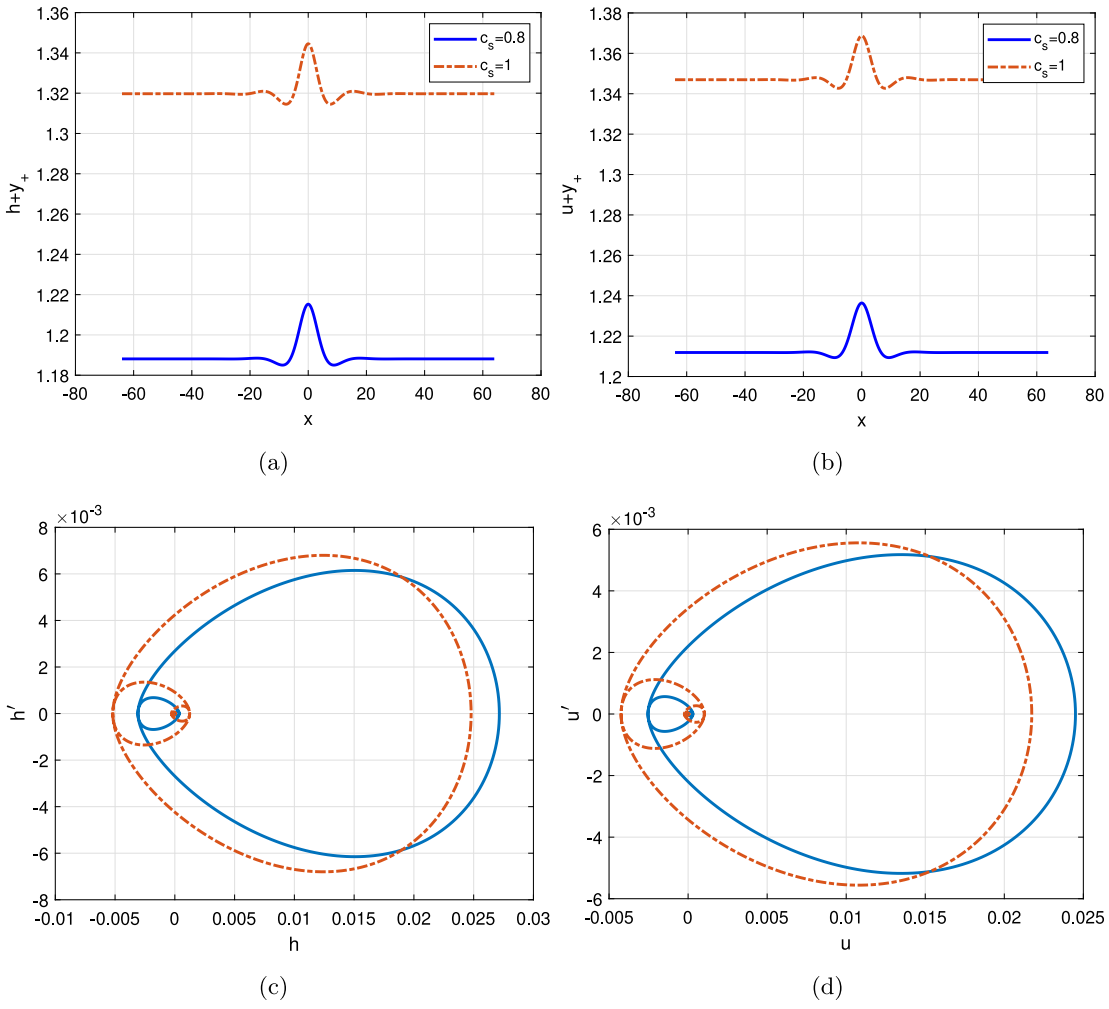

Fig. 5. Approximations to traveling wave solutions of (17) for two values of c_s. Case $g = g_-(c_s) - 10^{-4}$. (a) $\widetilde{h} + y_+$ profile; (b) $\widetilde{u} + y_+$ profile; (c) $\widetilde{h}$ phase plot; (d) $\widetilde{u}$ phase plot. Region 1 (left) of Fig. 1.

For the case under study, the numerical experiments of Section 5.3 found examples of the last two types.

Following the analysis above and making use of Lemmas 4.2–4.4, we will study and illustrate the dynamics of (34) with respect to each of the equilibria (29)

5.3. Dynamics around the equilibrium y_+

Recall that in this case, no region 3 of Fig. 1 is possible. Besides this, the analysis for the equilibrium y_+ leads to the following situations:

(i) Assume that $c_s > \frac{1}{2}$. In that case, we have three possibilities:

(i1) If $g < g_1^*(c_s)$, then $b_+ > 0$ and $\Delta_+ < 0$. The linearization matrix $L(c_s, y_+)$ has two symmetric couples of complex conjugate eigenvalues (region 1, right of Fig. 1). The numerical computations suggest the generation of classical traveling waves of elevation with a non-monotone behavior. For g close to $g_1^*(c_s)$, the profiles are smooth (cf. Fig. 3), developing some kind of peak at the point of maximum as g separates from $g_1^*(c_s)$.

(i2) When $g_1^*(c_s) \leq g < g_-(c_s)$, then $b_+ < 0$ and $\Delta_+ < 0$. The spectrum of the linearization corresponds to region 1, left, of Fig. 1. In Fig. 4, it is shown the persistence of the generation of classical traveling waves (of elevation) with non-monotone asymptotic behavior, as indicated in Section 5.2. Note that as $g \to g_-(c_s)$ then $\Delta_+ \to 0$ and we fall into the curve C_2, where the spectrum of the linearization changes to a double complex conjugate pair of imaginary eigenvalues. This seems to be reflected by a more oscillatory approach towards the equilibrium y_+ as $Z \to \pm\infty$, [18,40], see Fig. 5.

(i3) When $g_-(c_s) \leq g < g_1(c_s)$, then $b_+ < 0$ and $\Delta_+ > 0$ (region 4 of Fig. 1, where the spectrum has four imaginary eigenvalues, two by two conjugate). The behavior of the orbits as $g \to g_-$, described above, and the numerical computations (cf. Fig. 6) suggest that crossing from region 1 (left) to region 4 the dynamics changes from the generation of non-monotone traveling waves to periodic orbits in the form of periodic traveling waves, [19], cf. Section 5.2. As g approaches $g_1(c_s)$, we are approximating to the curve C_1, where the spectrum consists of two zero eigenvalues and two imaginary. The computations do not detect any modification in the nature of the generated profiles, although the amplitude of the emerging periodic traveling waves seems to decrease to zero and the solution tends to the constant state y_+.

(ii) Assume that $c_s < \frac{1}{2}$. In that case, $b_+ > 0$ (since $\gamma_+ < 0$) and we may have the following possibilities:

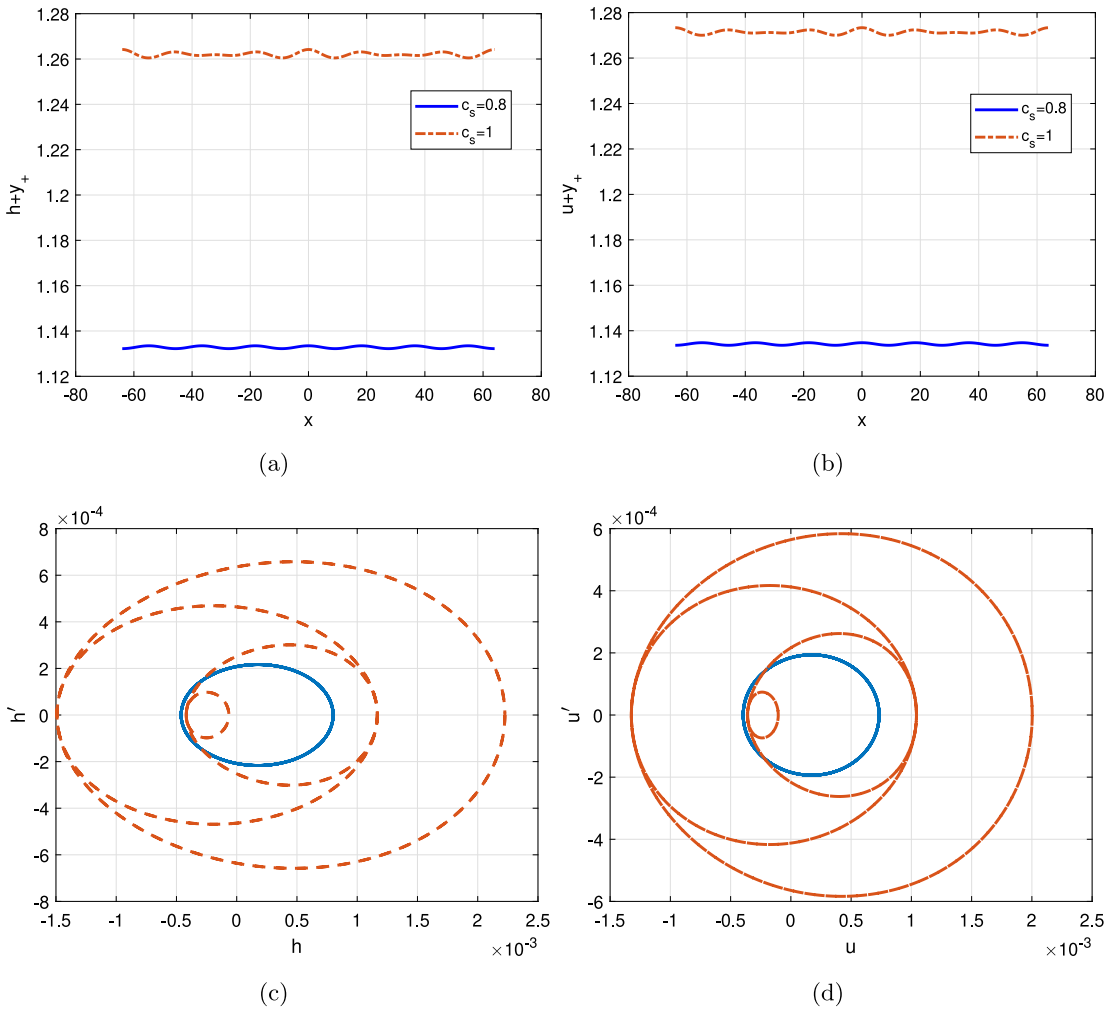

Fig. 6. Approximations to traveling wave solutions of (17) for two values of c_s. Case $g = g_-(c_s) + 10^{-6}$. (a) $\widetilde{h} + y_+$ profile; (b) $\widetilde{u} + y_+$ profile; (c) $\widetilde{h}$ phase plot; (d) $\widetilde{u}$ phase plot. Region 4 of Fig. 1.

(ii1) If $g < g_-(c_s)$ then $\Delta_+ < 0$ and this corresponds to region 1, right of Fig. 1: the linearization matrix $L(c_s, y_+)$ has four (symmetric) complex eigenvalues. The results are then similar to those obtained in (i1), where the homoclinic orbits correspond to non-monotone classical traveling waves. In this case, the profiles seem to be smoother as g approaches $g_-(c_s)$ (cf. Figs. 7 and 8).

(ii2) If $g_-(c_s) \le g < g_1(c_s)$ then $\Delta_+ > 0$ and we fall into region 2 of Fig. 1. When crossing from region 1 to region 2 and g goes from g_- to g_1 (approaching the curve C_0) there seems to be a change of type of homoclinic orbit (cf Figs. 9 and 10) with the generation of classical traveling waves with a monotone asymptotic behavior towards y_+, justified by the arguments in Section 5.2.

The results are summarized in Table 1.

Table 1
Bifurcation study of homoclinic orbits around the equilibrium y_+. NMTW (dep.): Non-monotone traveling wave of depression; MTW: Monotone traveling wave of depression; PTW: Periodic traveling wave.

$c_s > \frac{1}{2}(a_+ > 0)$	(b, a) region	Type of wave
$g < g_1^*(c_s)$	1R	NMTW (elev.)
$g_1^*(c_s) \le g < g_-(c_s)$	1L	NMTW (elev.)
$g_-(c_s) \le g < g_1(c_s)$	4	PTW
$c_s < \frac{1}{2}(a_+ > 0)$	(b, a) region	Type of wave
$g < g_-(c_s)$	1R	NMTW (elev.)
$g_-(c_s) \le g < g_1(c_s)$	2	MTW (elev.)

5.4. Dynamics around the equilibrium y_-

Recall that in this case regions 1, left, and 4 are not possible. A similar study for the equilibrium y_- leads to the following results.

(i) $c_s < \frac{1}{2}$. Here we may have four situations:

(i1) $g < g_+(c_s)$. Then $a_-, b_- > 0$, and $\Delta_- < 0$. Region 1, right.

(i2) $g_+(c_s) \le g < g_1^{**}(c_s)$. Then $a_-, b_- > 0$, and $\Delta_- > 0$. Region 2.

(i3) $g_1^{**}(c_s) \le g < g_1^*(c_s)$. Then $a_-, b_- < 0$. Region 3, left.

(i4) $g_1^*(c_s) \le g < g_1(c_s)$. Then $a_- < 0, b_- > 0$. Region 3, right.

(ii) $\frac{1}{2} < c_s < 3$. Here we may have the following:

(ii1) $g < g_+(c_s)$. Then $a_-, b_- > 0$, and $\Delta_- < 0$. Region 1, right.

(ii2) $g_+(c_s) \le g < g_1^{**}(c_s)$. Then $a_-, b_- > 0$, and $\Delta_- > 0$. Region 2.

(ii3) $g_1^{**}(c_s) \le g < g_1(c_s)$. Then $a_-, b_- < 0$. Region 3, left.

(iii) $c_s > 3$. Here we may have three subcases:

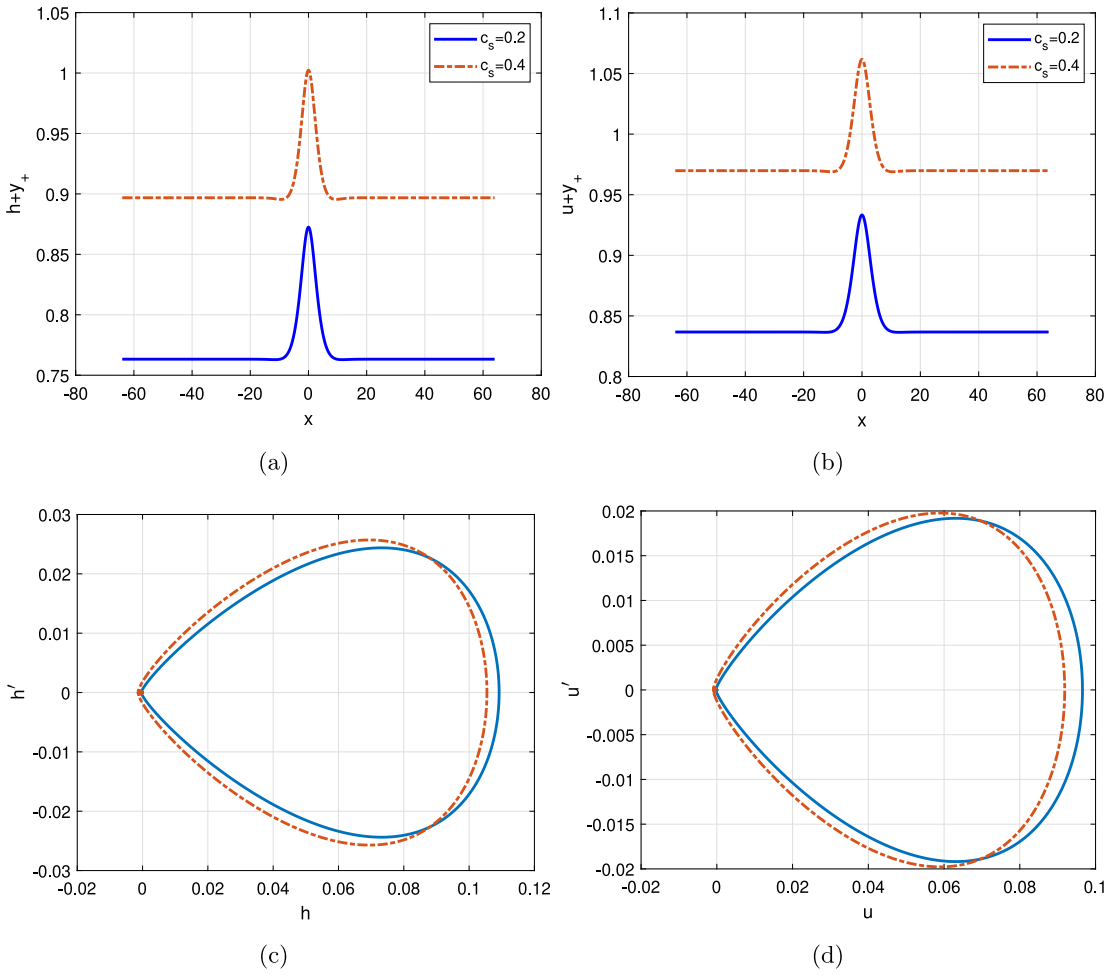

Fig. 7. Approximations to traveling wave solutions of (17) for two values of c_s. Case $g = g_-(c_s) - 0.001$. (a) $\widetilde{h} + y_+$ profile; (b) $\widetilde{u} + y_+$ profile; (c) $\widetilde{h}$ phase plot; (d) $\widetilde{u}$ phase plot. Region 1 (right) of Fig. 1.

(iii1) $g < g_+(c_s)$. Then $a_-, b_- > 0$, and $\Delta_- < 0$. Region 1, right.

(iii2) $g_+(c_s) \le g < g_1^{**}(c_s)$. Then $a_-, b_- > 0$, and $\Delta_- > 0$. Region 2.

(iii3) $g_1^*(c_s) \le g < g_1(c_s)$. Then $a_- < 0, b_- < 0$, and $\Delta_- > 0$. Region 3, left.

The types of the generated profiles corresponding to the homoclinic orbits with limit at y_- are summarized in Table 2. Compared to Table 1, several differences can be mentioned:

- The types of the emerging traveling waves in the regions do not depend on the range (i), (ii) or (iii) of the speed c_s.
- The non-periodic computed traveling waves are now of depression, cf. Section 5.2.
- In regions 1, right, and 2, classical traveling waves are computed. The h and u profiles seem to have a non-monotone behavior (more clearly observed in the first case) which seems to evolve to a monotone decay to the equilibrium y_- as g approaches $g_+(c_s)$, cf. Fig. 11. (Thus, (b_-, a_-) is closer to the curve C_3 and eventually crosses from region 1, right, to region 2.) The profiles develop a peak at the point where the maximum is attained, which is more pronounced and larger for larger speeds, as observed in Fig. 12. Note in this case that $y_- = 0$, and the computed traveling waves are solitary waves. A more rigorous proof of existence of such solitary waves may be considered by using classical approaches such as the concentration compactness theory of Lions, [41], or the positive operator theory, [42].

Table 2
Bifurcation study of homoclinic orbits around the equilibrium y_- TW (el.): Traveling waves of elevation; PTW: Periodic traveling waves.

$c_s < \frac{1}{2}$	(b, a) region	Type of wave
$g < g_1^+(c_s)$	1R	TW (dep.)
$g_+(c_s) \le g < g_1^{**}(c_s)$	2	TW (dep.)
$g_1^{**}(c_s) \le g < g_1^*(c_s)$	3L	TW-PTW
$g_1^*(c_s) \le g < g_1(c_s)$	3R	PTW
$\frac{1}{2} < c_s < 3$	(b, a) region	Type of wave
$g < g_+(c_s)$	1R	TW (dep.)
$g_+(c_s) \le g < g_1^{**}(c_s)$	2	TW (dep.)
$g_1^{**}(c_s) \le g < g_1(c_s)$	3L	TW-PTW
$c_s > 3 (a_+ > 0)$	(b, a) region	Type of wave
$g < g_+(c_s)$	1R	TW (dep.)
$g_+(c_s) \le g < g_1^{**}(c_s)$	2	TW (dep.)
$g_1^{**}(c_s) \le g < g_1(c_s)$	3L	TW-PTW

- Crossing from region 2 to region 3 (left) generates a change from computed classical traveling waves to periodic traveling waves, see Fig. 13. PTW's are also computed in region 3, right.
- A generalized traveling wave profile, predicted in Section 5.2 near C_1, is numerically generated in Fig. 14.

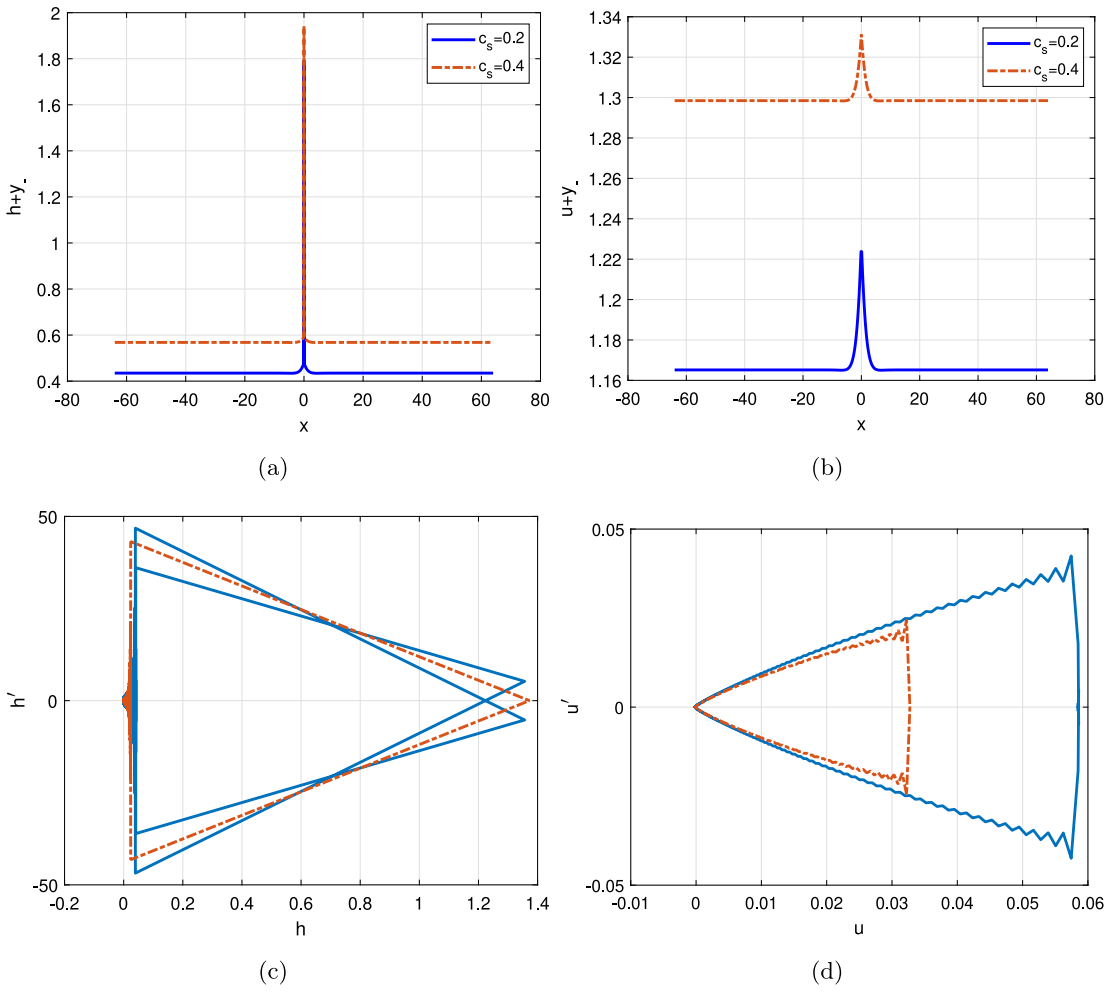

Fig. 8. Approximations to traveling wave solutions of (17) for two values of c_s. Case $g = g_-(c_s) - 0.001$. (a) $\widetilde{h} + y_+$ profile; (b) $\widetilde{u} + y_+$ profile; (c) $\widetilde{h}$ phase plot; (d) $\widetilde{u}$ phase plot. Region 1 (right) of Fig. 1.

6. Concluding remarks

The present paper is concerned with the existence of traveling wave solutions of the asymptotic model (5) for the evolution of a collision-free plasma in a magnetic field. In Section 3, using Crandall–Rabinowitz theorem [28] and the ideas in [14], we can rigorously prove the existence of traveling waves of small amplitude for (5).

Furthermore, from a reformulation of the model which involves only local terms, the corresponding ode system for the profiles of the traveling wave solutions is derived and the existence of equilibria is discussed in terms of the speed of the wave and a constant of integration g, playing the rôle in the corresponding bifurcation parameters. The structure of solutions around two of these equilibria can be studied from that of the solutions of an equivalent first-order system (34) around the origin as equilibrium. The reversible character of the system enables to analyze the dynamics from the application of normal form theory for reversible vector fields, [20], in related references, [18,21,22]. With this approach, and supported by an efficient numerical code to generate computed traveling wave profiles (described in Appendix), the emergence of several traveling waves is illustrated. The classification into the different regions depends on the speed on the waves and the constant g. The types of traveling wave solutions include classical traveling waves of monotone and non-monotone behavior, classical solitary waves (localized traveling waves), generalized traveling waves, and periodic traveling waves. In addition, some experiments suggest the convergence of peakon-type waves, cf. [29].

CRediT authorship contribution statement

Diego Alonso-Orán: Writing – review & editing, Writing – original draft, Methodology, Investigation, Conceptualization. **Angel Durán:** Writing – review & editing, Writing – original draft, Methodology, Investigation, Conceptualization. **Rafael Granero-Belinchón:** Writing – review & editing, Writing – original draft, Methodology, Investigation, Conceptualization.

Declaration of competing interest

The authors declare that they have no known competing financial interests or personal relationships that could have appeared to influence the work reported in this paper.

The authors whose names are listed immediately below certify that they have NO affiliations with or involvement in any organization or entity with any financial interest (such as honoraria; educational grants; participation in speakers' bureaus; membership, employment, consultancies, stock ownership, or other equity interest; and expert

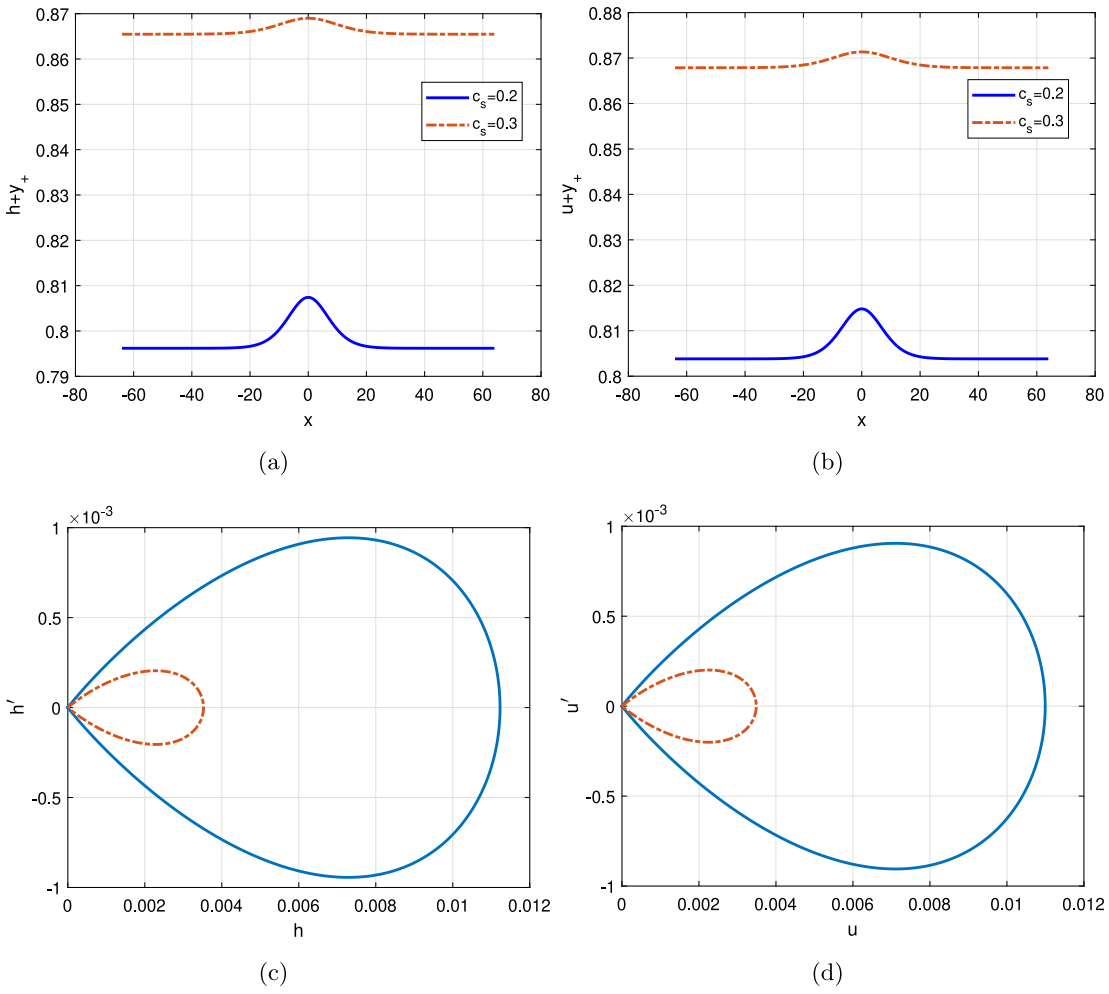

Fig. 9. Approximations to traveling wave solutions of (17) for two values of c_s. Case $g = g_-(c_s) + 10^{-6}$. (a) $\widetilde{h} + y_+$ profile; (b) $\widetilde{u} + y_+$ profile; (c) $\widetilde{h}$ phase plot; (d) $\widetilde{u}$ phase plot. Region 2 of Fig. 1.

testimony or patent-licensing arrangements), or non-financial interest (such as personal or professional relationships, affiliations, knowledge or beliefs) in the subject matter or materials discussed in this manuscript.

Acknowledgments

The authors gratefully acknowledge Claudia García for fruitful discussions regarding bifurcation theory and Daniel Sánchez-Simón del Pino for pointing out the reference of Lemma 2.1. D.A-O has been partially supported by RYC2023-045563-I (MICIU/AEI/10.13039/501100011033 and FSE+) and the project PID2023-148028NB-100. D.A-O and R. G-B are also supported by the project "Análisis Matemático Aplicado y Ecuaciones Diferenciales" Grant PID2022-141187NB-I00 funded by MCIN/AEI and acronym "AMAED". This paper is part of the project PID2022-141187NB-I00 with acronym *AMAED* funded by MICIU/AEI/10.13039/501100011033 and by FEDER, UE/AEI/10.13039/501100011033/FEDER, UE. A.D. is supported by the Spanish Agencia Estatal de Investigación under Research Grant PID2023-147073NB-100.

Appendix. A procedure for the numerical generation of traveling waves

The numerical method to approximate solutions of (33) is here formulated. The procedure is based on the reduction to the case $g = 0$ considered in Section 4.1. The equation is first written in fixed-point form

$$\mathcal{L}\widetilde{u} = \mathcal{N}(\widetilde{u}), \tag{53}$$

(we occasionally recover the tilde in the notation, for reasons that will become evident below) where $\mathcal{L}$ is a linear operator and $\mathcal{N}(\widetilde{u})$ gathers for the nonlinear terms involving $\widetilde{u}$ and its derivatives up to fourth order. Explicitly

$$\mathcal{L} = \alpha_{\pm}\mathcal{J}^2 + \frac{y_{\pm}}{2}\partial_x^2 - \frac{1}{2}\mathcal{J},$$
$$\mathcal{N}(\widetilde{u}) = -\frac{1}{2}\left(\frac{3}{2}\mathcal{J}(\mathcal{J}\widetilde{u})^2 + \partial_x(\widetilde{u}_x\mathcal{J}\widetilde{u}) - \frac{1}{2}\mathcal{J}(\widetilde{u}_x^2)\right).$$

Eq. (53) is iteratively solved from an approximation to (33) on a long enough interval with periodic boundary conditions given by a Fourier collocation method. Let $N \geq 1$ be an even integer and let

$$x_j = -l + j\Delta x, \quad j = 0, \dots, N-1, \Delta x = 2l/N, \tag{54}$$

be a uniform grid of collocation points on $(-l, l)$. We consider the finite dimensional space

$$S_N = \text{span}\{e^{ik\pi(x+l)/l}, k \in \mathbb{Z}, -\frac{N}{2} \leq k \leq \frac{N}{2} - 1\},$$

and define the spectral Fourier collocation approximation to a solution $\widetilde{u}$ of the periodic problem associated to (33) on $(-l, l)$ as $\widetilde{u}^N \in S_N$ satisfying (53) at the collocation points (54). The approximation $\widetilde{u}^N$ is typically represented by the nodal values

$$\widetilde{u}_\Delta = (\widetilde{u}_0, \dots, \widetilde{u}_{N-1})^T, \tag{55}$$

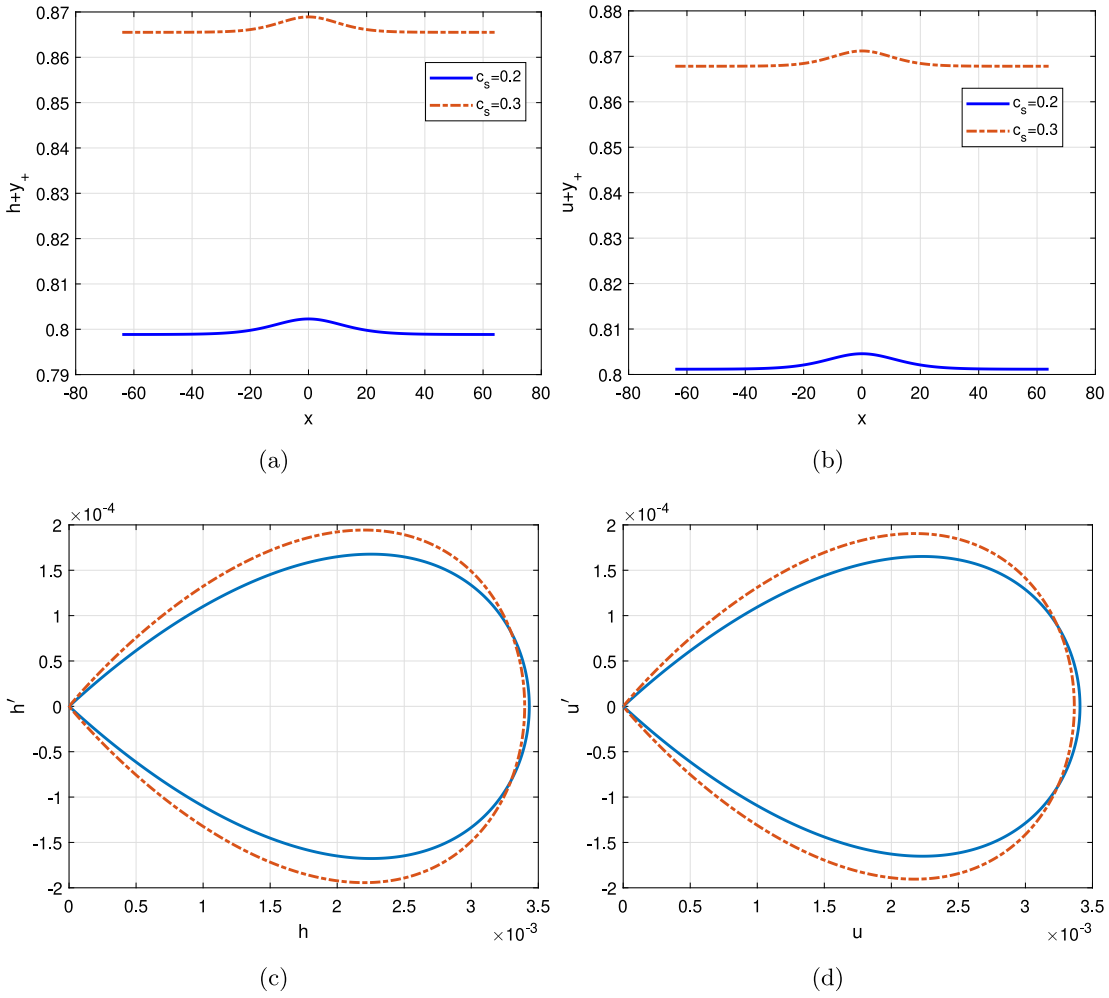

Fig. 10. Approximations to traveling wave solutions of (17) for two values of c_s. Case $g = g_1(c_s) - 10^{-6}$. (a) $\widetilde{h} + y_+$ profile; (b) $\widetilde{u} + y_+$ profile; (c) $\widetilde{h}$ phase plot; (d) $\widetilde{u}$ phase plot. Region 2 of Fig. 1.

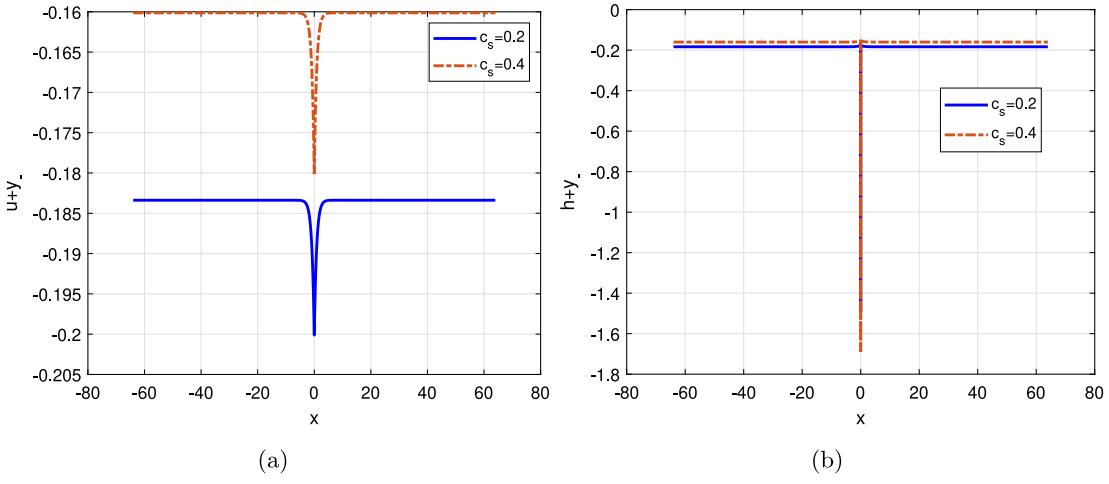

Fig. 11. Approximations to traveling wave solutions of (17) for two values of c_s. Case $g = g_+(c_s) - 0.1$. (a) $\widetilde{h} + y_-$ profile; (b) $\widetilde{u} + y_-$ profile. Region 1 (right) of Fig. 1.

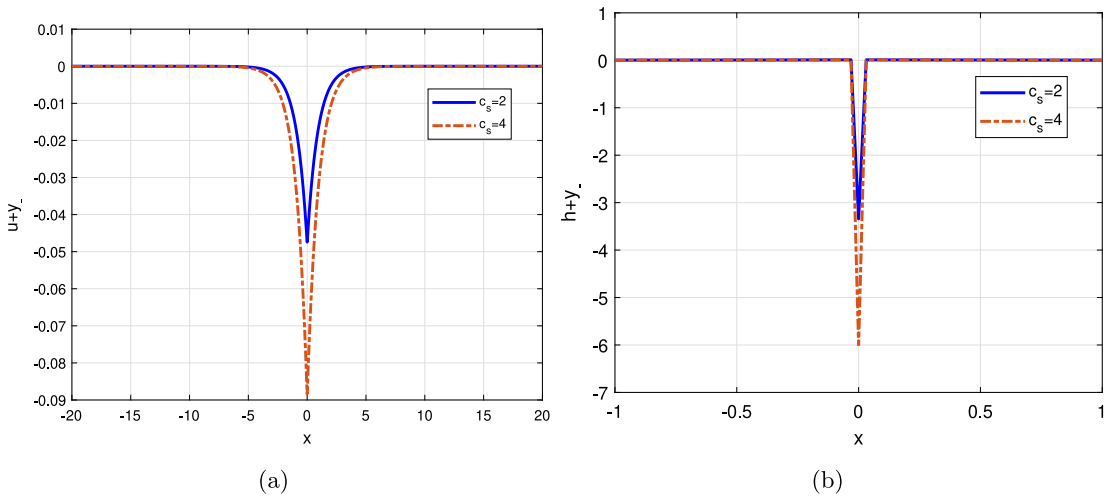

Fig. 12. Approximations to traveling wave solutions of (17) for two values of c_s. Case $g = 0$. (a) $\widetilde{h} + y_-$ profile; (b) $\widetilde{u} + y_-$ profile. Region 2 of Fig. 1.

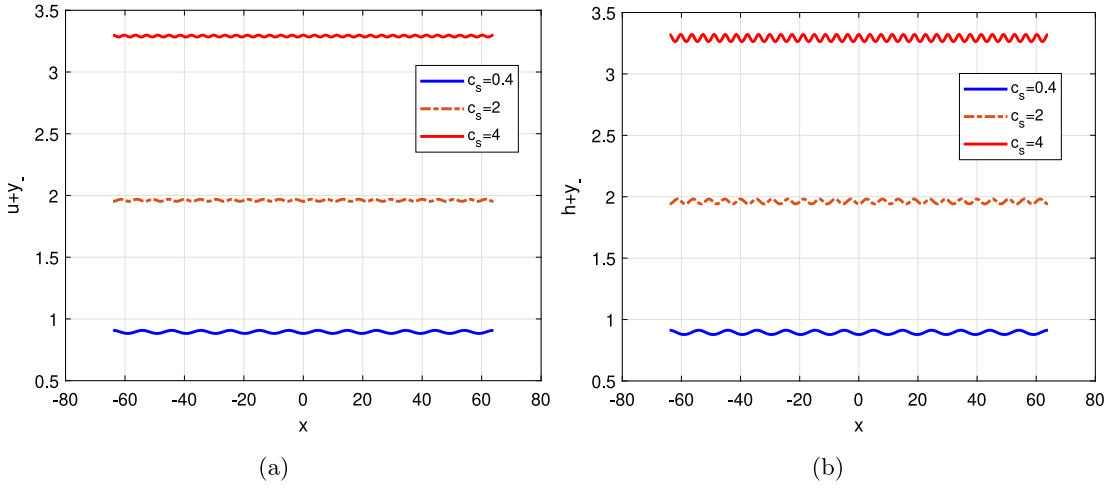

Fig. 13. Approximations to traveling wave solutions of (17) for two values of c_s. Case $g = g_1(c_s) - 0.001$. (a) $\widetilde{h} + y_-$ profile; (b) $\widetilde{u} + y_-$ profile. Region 3 (right) of Fig. 1.

with $\widetilde{u}_j = \widetilde{u}^N(x_j), j = 0, \dots, N-1$ as approximations to the nodal values of the solution $\widetilde{u}(x_j)$. Thus the algebraic system satisfied by (55) is of the form

$$\mathcal{L}_\Delta \widetilde{u}_\Delta = \mathcal{N}_\Delta(\widetilde{u}_\Delta), \tag{56}$$

where

$$\begin{aligned}\mathcal{L}_\Delta &= \alpha_\pm (I_N - D_N^2)^2 + \frac{y_\pm}{2} D_N^2 - \frac{1}{2}(I_N - D_N^2),\\ \mathcal{N}_\Delta(\widetilde{u}_\Delta) &= -\frac{1}{2}\left(\frac{3}{2}(I_N - D_N^2)((I_N - D_N^2)\widetilde{u}_\Delta).^2 + D_N(D_N\widetilde{u}_\Delta.(I_N - D_N^2)\widetilde{u}_\Delta)\right.\\ &\quad \left. -\frac{1}{2}(I_N - D_N^2)((D_N\widetilde{u}_\Delta).^2)\right).\end{aligned}$$

where I_N denotes the $N \times N$ identity matrix, D_N stands for the pseudospectral differentiation matrix, [43], and the dots in the nonlinear part $\mathcal{N}_\Delta(\widetilde{u}_\Delta)$ denotes Hadamard products of the corresponding vectors. The fixed-point system (56) is implemented by writing its Fourier representation (in terms of the discrete Fourier components of the vectors (55) via Discrete Fourier Transform) and solving iteratively the resulting algebraic system. A typical iterative resolution consists of combining the Petviashvili method with a vector extrapolation technique to accelerate the convergence. The details can be seen in e. g. [44] and references therein.

After obtaining approximations $\widetilde{u}_\Delta$ to the profile $\widetilde{u}$ solution of (33), then we compute $u_\Delta = \widetilde{u}_\Delta + y$ to approximate (19) for both $y = y_\pm$ and, finally, we approximate the h profile from the discrete version of (15)

$$h_\Delta = (I_N - D_N^2)u_\Delta.$$

In order to illustrate the accuracy of the method, Fig. 15 shows the Euclidean norm of the error in the residual

$$\mathcal{L}_\Delta u^{[\nu]} - \mathcal{N}_\Delta(u^{[\nu]}), \tag{57}$$

as function of the number ν of iterations for the numerical generation of the profiles of Fig. 3.

Data availability

No data was used for the research described in the article.

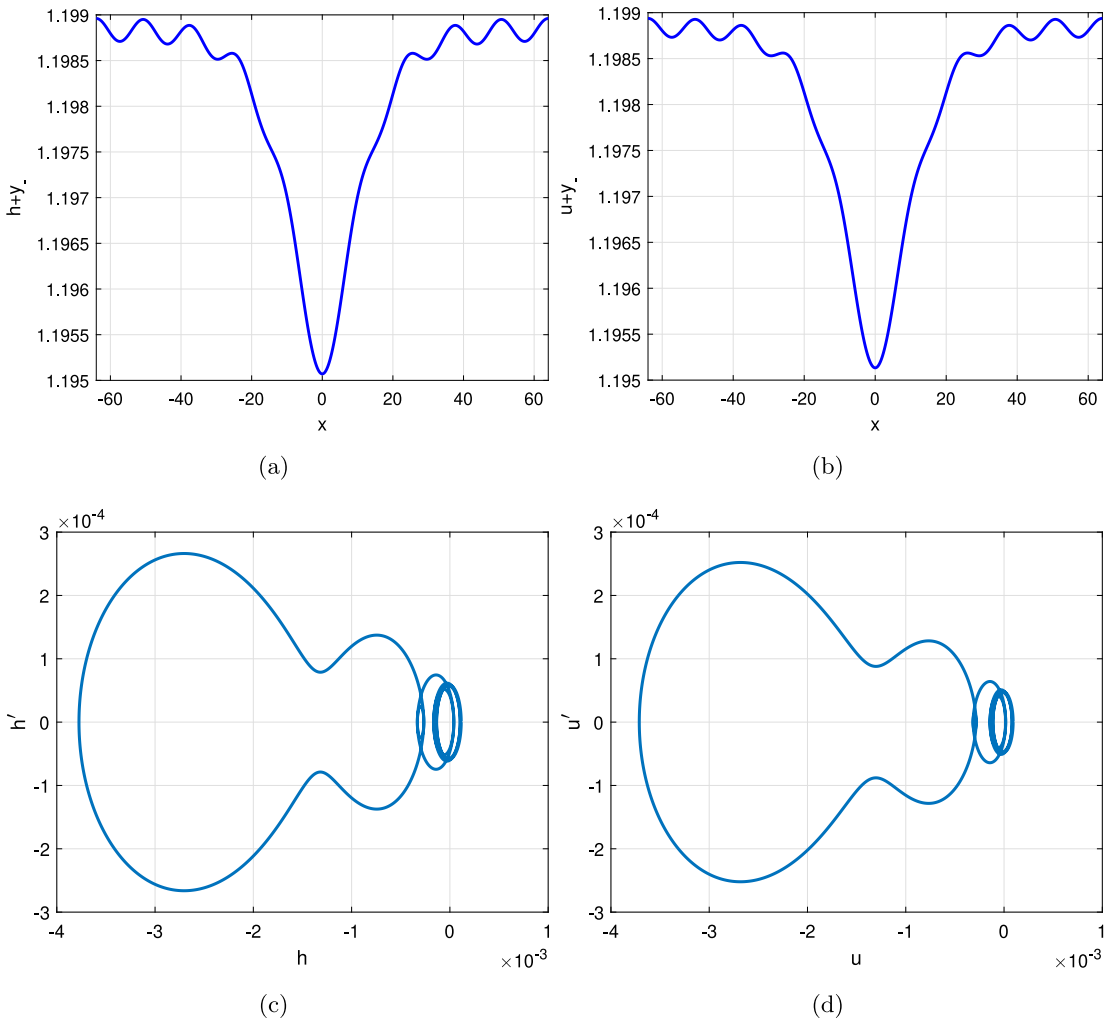

Fig. 14. Approximations to traveling wave solutions of (17) for $c_s = 0.8$. Case $g = g_1(c_s) - 10^{-6}$. (a) $\widetilde{h} + y_-$ profile; (b) $\widetilde{u} + y_-$ profile; (c) $\widetilde{h}$ phase plot; (d) $\widetilde{u}$ phase plot. Region 1 (right) of Fig. 1.

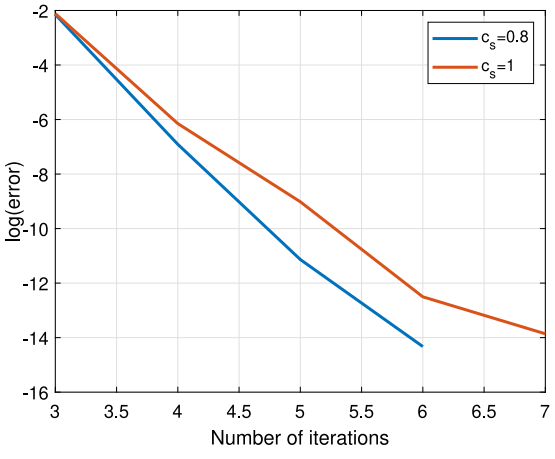

Fig. 15. Euclidean norm of the error (57) in the numerical generation of the profiles from Fig. 3 (semilog scale).

References

[1] Y.A. Berezin, V. Karpman, Theory of nonstationary finite-amplitude waves in a low-density plasma, Sov. Phys. JETP 19 (1964) 1265–1271.

[2] C. Gardner, G. Morikawa, Similarity in the Asymptotic Behaviour of Collision-Free Hydromagnetic Waves and Water Waves, Tech. rep., New York Univ. New York. Inst. of Mathematical Sciences, 1960.

[3] T. Kakutani, H. Ono, T. Taniuti, C.-C. Wei, Reductive perturbation method in nonlinear wave propagation ii, Appl. Hydromagn. Waves Cold Plasma J. Phys. Soc. Jpn. 24 (5) (1968) 1159–1166, (1968).

[4] X. Pu, M. Li, KdV limit of the hydromagnetic waves in cold plasma, Z. Angew. Math. Phys. 70 (1) (2019) 32, 2019.

[5] D. Alonso-Orán, R. Granero-Belinchón, Well-posedness for an hyperbolic–hyperbolic–elliptic system describing cold plasmas, Appl. Math. Lett. 147 (2024).

[6] J. Bae, J. Choi, B. Kwon, Singularity formation of hydromagnetic waves in cold plasma, 2024, arXiv:2407.18619.

[7] D. Alonso-Orán, A. Durán, R. Granero-Belinchón, Derivation and well-posedness for asymptotic models of cold plasmas, Nonlinear Anal. 244 (2024) 113539.

[8] A. Scott, Nonlinear science, in: Emergence and Dynamics of Coherent Structures, Oxford Univ. Press, 1999.

[9] B. Sandstede, Stability of traveling waves, in: (B. Fiedler (Ed.), Handbook of Dynamical Systems, North-Holland, 2002, pp. 983–1055.

[10] J.L. Bona, On solitary waves and their role in the evolution of long waves, Appl. Nonlinear Anal. Phys. Sci. (1981) 183–205.

[11] T.H. Stix, Waves in Plasma, American Institute of Physics, NY, 1997.

[12] R. Dumond, Waves in Plasmas, France, 2017, p. 117, cel-01463091.

[13] A. Decoster, Nonlinear travelling waves in a homogeneous cold collisionless plasma, Phys. Rep. 47 (5) (1978) 285–422.

[14] D. Alonso-Orán, C. García, R. Granero-Belinchón, Traveling gravity-capillary waves with odd viscosity, 2024, arXiv preprint arXiv:2407.19743.

[15] A. Constantin, E. Varvaruca, Steady periodic water waves with constant vorticity: regularity and local bifurcation, Arch. Ration. Mech. Anal. 199 (2011) 33–67.

[16] J. Lenells, Traveling wave solutions of the Camassa–Holm and Korteweg–de Vries equations, J. Nonlinear Math. Phys. 11 (2004) 508–520.

[17] Lenells J., Traveling wave solutions of the Camassa–Holm equation, J. Differential Equations 217 (2005) 393–430.
[18] A.R. Champneys, Homoclinic orbits in reversible systems and their applications in mechanics, Fluids Opt. Phys. D 112 (1988) 158–186.
[19] G. Iooss, K. Kirchgässner, Water waves for small surface tension: an approach via normal form, Proc. Roy. Soc. Edinb. A 112 (1992) 267–299.
[20] M. Haragus, G. Iooss, Local Bifurcations, Center Manifolds, and Normal Forms in Infinite-Dimensional Dynamical Systems, Springer London Dordrecht Heidelberg New York, 2011.
[21] A.R. Champneys, A. Spence, Hunting for homoclinic orbits in reversible systems: A shooting technique, Adv. Comput. Math. 1 (1993) 81–108.
[22] A.R. Champneys, J.F. Toland, Bifurcation of a plethora of multi-modal homoclinic orbits for autonomous Hamiltonian systems, Nonlinearity 6 (1993) 665–772.
[23] V.A. Dougalis, A. Durán, L. Saridaki, On solitary-wave solutions of Boussinesq/Boussinesq systems for internal waves, Phys. D 428 (2021) 133051.
[24] E. Stein, Singular Integrals and Differentiability Properties of Functions (PMS-30), Princeton University Press, 1970.
[25] H. Abels, Pseudo-Differential and Singular Integral Operators: An Introduction with Applications, Boston: De Gruyter, Berlin, 2012, https://doi.org/10.1515/9783110250312.
[26] T. Kato, Perturbation Theory for Linear Operators, Springer-Verlag Berlin-Heidelberg-New York, 1995.
[27] H. Kielhöfer, Bifurcation Theory: An Introduction with Applications To PDEs, Springer-Verlag, Berlin- Heidelberg-New York, 2004.
[28] M.G. Crandall, P.H. Rabinowitz, Bifurcation from simple eigenvalues, J. Funct. Anal. 8 (1971) 321–340.
[29] J. Zhou, L. Tian, Solitons, peakons and periodic cusp wave solutions for the Fornberg-Whitham equation, Nonlinear Anal. 11 (2010) 356–363.
[30] S. Wiggins, Introduction To Applied Nonlinear Dynamical Systems and Chaos, Springer, New York, 1990.
[31] G. Iooss, A codimension 2 bifurcation for reversible vector fields, Fields Inst. Comm. 4 (1995) 201–217.
[32] S. Roy Choudhury, Solitary-wave families of the Ostrovsky equation: An approach via reversible systems theory and normal forms, Chaos Solitons Fractals 33 (2007) 1468–1479.
[33] A. Durán, G.M. Muslu, On solitary-wave solutions of rosenau-type equations, Commun. Nonlinear Sci. Numer. Simul. 137 (2024) 108130.
[34] E. Lombardi, Oscillatory Integrals and Phenomena beyond All Algebraic Orders, Springer-Verlag, Berlin-Heidelberg, 2000.
[35] A.R. Champneys, B.A. Malomed, Moving embedded solitons, J. Phys. A 32 (1999) 547–553.
[36] G. Iooss, M. Adelmeyer, Topics in Bifurcation Theory and Applications, second ed., World Scientific, Singapore, 1999.
[37] G. Iooss, M.C. Peroueme, Perturbed homoclinic solutions in reversible 1 : 1 resonance vector fields, J. Differential Equations 102 (1993) 62–88.
[38] F. Dias, G. Iooss, Water waves as a spatial dynamical system, in: Serre D Friedlander S (Ed.), Handbook of Mathematical Fluid Dynamics, Elsevier, Amsterdam, 2003, pp. 443–499, [Chapter 10].
[39] J. Härterich, Cascades of reversible homoclinic orbits to a saddle-focus equilibrium, Phys. D 112 (1997) 187–200.
[40] V.A. Dougalis, A. Durán, D.E. Mitsotakis, Numerical approximation of solitary waves of the benjamin equation, Math. Comp. Simul. 127 (2016) 56–79.
[41] P.L. Lions, The concentration-compactness principle in the calculus of variations. The locally compact case, Part I Part II. Ann. Inst. Henri PoincarÉ Sect A (N. S.) 1 (1984) 109–145, 223–283.
[42] T.B. Benjamin, J.L. Bona, D.K. Bose, Solitary-wave solutions of nonlinear problems, Philos. Trans. R. Soc. Lond. A 331 (1990) 195–244.
[43] C. Canuto, M.Y. Hussaini, A. Quarteroni, A.T. Zang, Spectral Methods in Fluid Dynamics, Springer, New York, 1985.
[44] V.A. Dougalis, A. Durán, L. Saridaki, Numerical solution of internal-wave systems in the intermediate long wave and the benjamin–ono regimes, Bull. Hell. Math. Soc. 66 (2022) 11–25.